JOURNAL OF MULTIFUNCTIONAL MATERIALS & PHOTOSCIENCE
8(2), December 2017, pp. 205-236

# A Review on New Developments In 3D Graphene Based Polymer Composites

**Biswas Md Rokon Ud Dowla[1] and Won-Chun Oh[1*]**

[1]*Department of Advanced Materials Science & Engineering, Hanseo University, Seosan-si, Chungnam, Korea, 356-706*

***Abstract:*** Integration of graphene with polymers to construct three-dimensional porous graphene/polymer composites (3DGPCs) have attracted considerable attention in the past few years for both the fundamental studies and diverse technological applications. With the broad diversity in molecular structures of graphene and polymers via rich chemical routes, a number of 3DGPCs have been developed with unique structural, electrical, mechanical properties, chemical tenability and attractive functions, which greatly expands the research horizon of graphene-based composites. In particular, the properties and functions of the 3DGPCs can be readily tuned by precisely controlling the hierarchical porosity in the 3D graphene architecture as well as the intricate synergistic interactions between graphene and polymers. In this article, we review the recent progress in 3DGPCs, including their synthetic strategies and potential applications in environmental protection, energy storage, sensors and conducting composites. Lastly, we will conclude with a brief perspective on the challenges and future opportunities.

***Keywords:*** graphene, polymer, three-dimensional, composites, environment, energy, sensor

## Introduction

Graphene, a single or few atomic layer of carbon lattices in honeycomb structure, has attracted intense interest due to its extraordinary physical and chemical properties, including excellent electronic conductivity, superior mechanical properties, and enormous theoretical specific surface area (2630 m2 g- 1).[1-5]As a versatile building block, graphene has been widely used to prepare macroscopic threedimensional (3D) frameworks such as hydrogels/aerogels, foams, and sponges via diverse synthetic strategies, including self-assembly of chemically converted graphene nanosheets, 6-9 chemical vapor deposition (CVD), [10, 11] thermolytic cracking, [12-15] and in situ unzipping carbon nanotubes, [16,17] etc. [18,19] Theresulted three-dimensional graphene frameworks (3DGFs) typically exhibit extremely low density and highly interconnected hierarchical porous structure, which enable easy access and diffusion of various ions and molecules. With little restacking of the graphene sheets, the 3DGFs largely retain the intrinsic surface and other advantageous properties of individual graphene sheets, which is critical for achieving the

*Corresponding author*: wc_oh@hanseo.ac.kr*

maximum functionality of the graphene-based macroscopic materials for practical applications in various fields such as energy storage[,20-22] catalysis,[23,24] sensing and separation.[25-27] Recently, incorporating polymers with graphene to construct functional 3D graphene/polymer composites (3DGPCs) have gained increasing attention for not only understanding the fundamental self-assembly chemistry between graphene and polymers, but also expanding the functions and applications of 3DGFs.28-33 Tremendous efforts have been devoted to the development of synthetic methods for 3DGPCs with various morphologies, structures and properties, in order to satisfy the requirements arising from different applications. Here we review recent advances in the synthesis, properties and applications of 3DGPCs, and discuss the future challenge and opportunities of 3DGPCs.

**Synthetic Strategies**

In most synthetic strategies for construction of 3DGPCs, graphene oxide (GO) is a commonly used precursor because of its characteristic of low-cost and high-throughput production and easy conversion to reduced graphene oxide (rGO).34 In general, the synthetic strategies of 3DGPCs involving GO precursor could be roughly divided into three categories: (i) assembly of GO sheets with polymers, (i) directly incorporating polymers during reduction self-assembly of GO sheets, (i) incorporating polymers into pre-synthesized 3DGFs. The morphology and synthetic routes of 3DGPCs are illustrated in Figure 1. The following subsections will discuss these methods and the corresponding produced 3DGPCs in detail.

**Assembly of GO sheets with polymers**

Owing to the presence of various hydrophilic oxygenated functional groups such as hydroxyl, carboxyl, and epoxy groups, GO sheets can be easily dispersed in many polar solvents, especially in water, at high concentrations.35,36 Thus, the assembly of GO sheets with polymers as the cross-linker in organic or aqueous media can readily produce 3D GO/polymer composite gels which then can be readily converted into 3D rGO/polymer composite gels by chemical reduction. In this strategy, GO sheets can be not only regarded as carbon nanomaterials but also acted like 2D macromolecules that are decorated by a large number of highly reactive oxygen-containing functional groups. The formation of the 3D composite gels relies on the cross-linking effect between GO sheets and polymer chains through either covalent bonds and/or non-covalent interactions.37,38 As an example of covalent cross-linking, Hughes's group fabricated a stable 3D GO/ poly(oxypropylene) diamines (D400) composite gel by exploiting epoxy groups on the surface of GO in a ring opening reaction with amine groups of D400.39 Compared with covalent cross-linking methods, the non-covalent methods such as hydrogen bonding, electrostatic interaction and π-π stacking, are mostly frequently used to prepare 3DGPCs since graphene's natural structure is unaffected. Moreover, non-covalent methods are reversible in some cases, which could be more desirable for retaining graphene's intrinsic properties or creating graphene-based smart composites.40 Among these interactions, hydrogen bonding is a usual driving force for supramolecular assembly, and the assembly

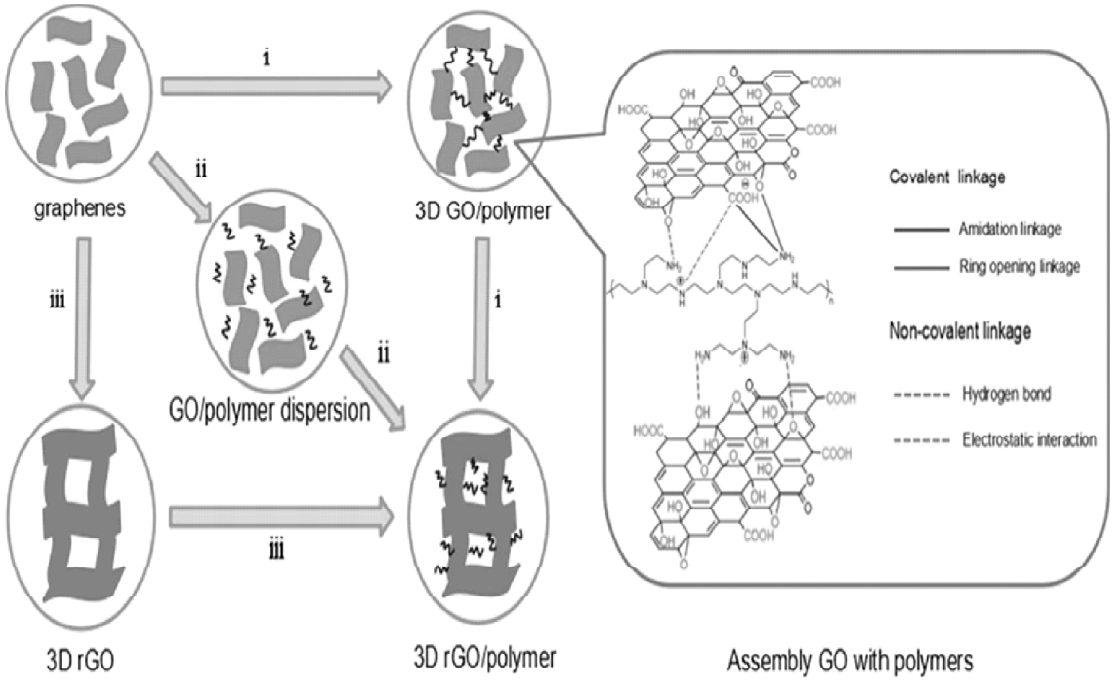


**Figure 1:** Schematic illustration of synthetic methods for 3DGPCs started from GO precursor. i) Assembly of GO sheets with polymers as cross-linkerÿinset shows the assembly of GO sheets with polyethylenimine (PEI) by covalent linkage and/or non- covalent interactions.). (?) Directly mixing the solutions of polymer or its precursor with GO to achieve uniform dispersion, followed by a reduction self-assembly of GO. (?) Self-assembly of GO at first, and then incorporating polymers into the pre-synthesized 3DGFs

of GO with polymers induced by hydrogen bonding has been realized in many systems. For examples, poly(vinyl alcohol) (PVA), poly (ethylene oxide) (PEO), poly (vinyl pyrrolidone) (PVP), hydroxypropylcellulose (HPC), etc., can form hydrogen bonds with adjacent GO sheets, resulting in a cross-linking network and forming a composite hydrogel.41-45 Electrostatic interaction is also an another important driving force for the assembly of GO or rGO sheets with polymers. GO or rGO sheets are negatively charged due to the ionized oxygen-containing functional groups, which can be used to assembly with positively charged polymers through electrostatic interactions. Typically, polydimethyldiallylammonium chloride (PDDA) can be an efficient cross-linker for 3D assembly with GO by electrostatic interaction between the quaternary ammonium groups of PDDA and carboxyl groups of GO sheets.[44] It has also been confirmed that electrostatic interaction is more effective than hydrogen bonding for the 3D assembly process because the critical gel concentration in the hydrogen bonding system is higher than that in electrostatic interaction system, likely due to the longer range electrostatic interactions when compared with hydrogen bonding interaction. There are now a number of biopolymers, such as DNA,46 chitosan (CHI),47 cellulose,48 sodiumalginate (SA),49 collagen, 50 *et al.* that have been demonstrated to be suitable for preparation of 3D GO/

polymer composite hydrogels. Taking an example of DNA,46 3D GO/DNA hydrogel can be prepared by mixing the GO dispersion and the aqueous solution of double-stranded DNA (dsDNA) followed by heating the omogeneous mixture at 90p! for 5 min. During the heating process, the dsDNA was unwound to single-stranded DNA (ssDNA) and then in situ formed ssDNA chains bridged adjacent GO sheets via strong non-covalent interactions, including the π-π stacking and hydrophobic interactions between the bases of DNA and graphitic domain of GO, as well as the electrostatic/hydrogen bonding interactions between the prime amines of bases and the oxygen-containing groups of GO. As shown in Figure 2, a self-assembled composite hydrogel of GO sheets and ssDNA chains was formed, and the hydrogel has a well-defined and interconnected 3D porous network. The pore diameters range from submicrometer to several micrometers and the pore walls consist of very thin layers of stacked GO sheets. The 3D GO/DNA composite hydrogel was stable in a variety of harsh conditions, such as in strong acidic (pH 2), basic

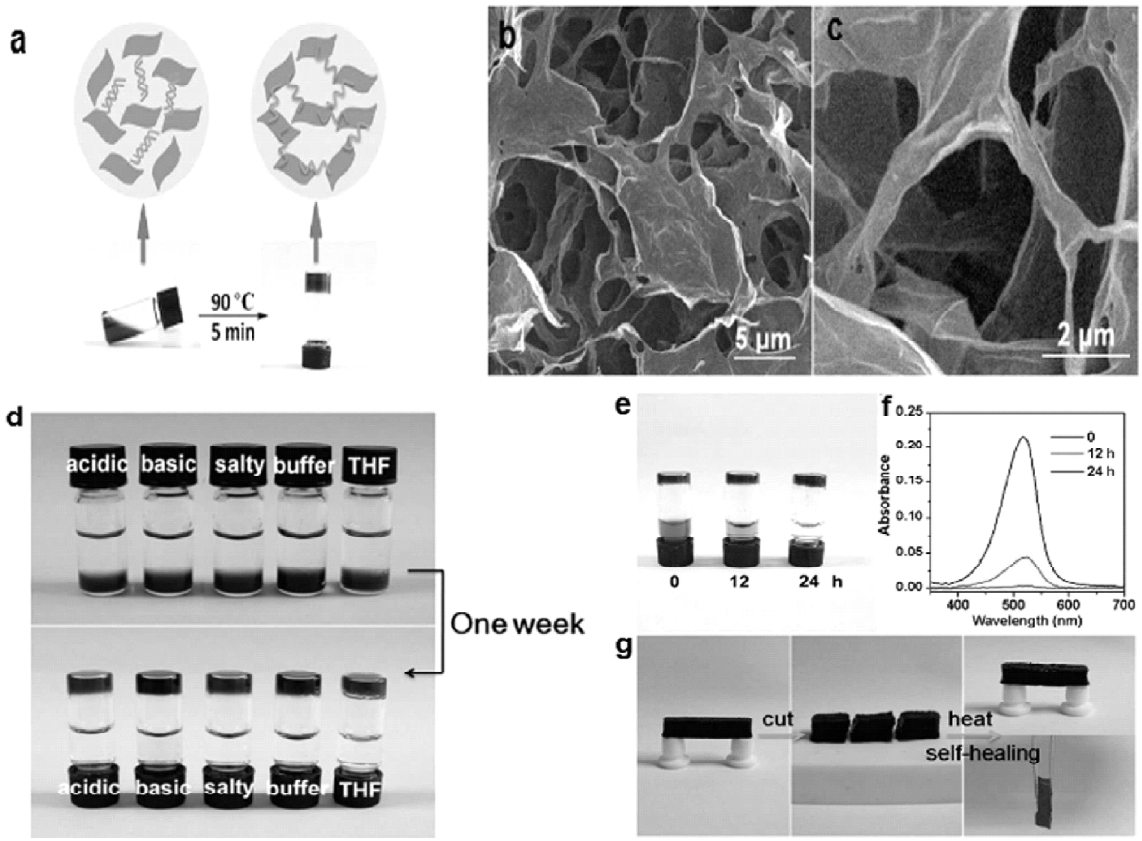


**Figure 2:** (a) The procedure of preparing 3D GO/DNA composite hydrogel and the proposed self-assembly gelation mechanism. (b and c) SEM images with low and high magnifications of the hydrogel's microstructures. (d) Effects of pH, NaCl, buffer, and organic solvent on the hydrogel's stability. Photographs (e) and absorption spectra (f) of an aqueous solution of safranine O after adsorption by 3D GO/DNA hydrogel for different times. (g) Self-healing process of 3D GO/DNA composite hydrogel. Reproduced with permission from ref.46. Copyright 2010 American Chemical Society

(pH 13), or salt (1M NaCl) aqueous solution, or even in organic solvents such as tetrahydrofuran (THF). In addition, the as-prepared 3D GO/DNA hydrogel exhibited high dye-adsorption capacity and attractive self-healing function.

**Directly incorporating polymers during reduction self-assembly of GO**

Reduction self-assembly of GO is an effective way to drive the cross-link of chemically concerted graphene sheets via partial π-π stacking interaction to form a 3D interconnected porous structure.51-55 Direct incorporation of polymers during the reduction self-assembly process is a convenient way to 3DGPCs and has gained increasing attention because these polymers not only render 3DGPCs with superior performance and characteristic, but also act as spacers to further minimize the agglomeration of graphene sheets. The approaches generally involve directly mixing the solutions of polymer or its precursor with GO to achieve uniform dispersion, followed by a reduction process to obtain the 3DGPC structures. For example, Li's group fabricated 3D rGO/polyimide (PI) composites by introducing water-soluble PI during the reduction selfassembly of GO triggered by a thermal annealing process.56 The overall preparation procedure was illustrated in Figure 3a. Firstly, GO solution and poly (amic acid) solution (PAA, water-soluble PI precursor) were mixed together, and then the mixture was further treated by a cyrodesiccation method.

Finally, the resulting monolith was subjected to a thermal annealing process at 300 p! to form a 3D rGO/PI porous architecture. The PAA can attach on the surfaces of GO sheets through hydrogen bonding, which effectively promote the incorporation of polymers and alleviate the self-stacking of graphene during the assembly process. Recently, nanostructured polymers, such as nanofibers,57 nanorods,58 nanotubes,59 nanowires,60 have also been designed to incorporate with GO that was then self-assembled into 3DGPCs through a reduction route. For instance, Bao's group introduced pre-prepared polyaniline (PANI) nanowires into GO aqueous dispersion.60 As shown in Figure 3b, PNAI nanowires may interact with more than one neighboring GO sheets via ð-ð stacking and hydrogen bonding interactions. Thus, upon the hydrothermal reduction, PANI nanowires were successfully wrapped into graphene layers during the 3D self-assembly of rGO and served as spacers to prevent graphene from restacking and agglomeration. On the surfaces of rGO sheets by electropolymerization at positive potential.62 Additionally, considering that the aniline can be polymerized *via* oxidization under an acidic condition using a variety of oxidants, and GO sheets can be chemically reduced into rGO by certain reductant including aniline, 3D rGO/PANI composites have also been prepared through one-step *in situ* redox reaction between GO and aniline. The redox reaction can take place instantly at room temperature.63 In another similar case, Sun *et al.* developed 3D rGO/PPy hybrid aerogel by a spontaneous assembly (*i.e. in situ* redox ) method in the absence of any other reductant or oxidizing agent at room temperature (Figure 3c).64 The redox reaction between GO and Py resulted in reduction of GO and polymerization of Py in the meantime. Thus, onestep assembly through redox reaction of monomers and GO is environmentally friendly, low cost, and easy to scale-up. For non-polar, highly viscous or cross-linked polymers, due to the absence of interfacial interaction between polymers and graphene, it

is challenging to form uniform dispersion of polymers with GO and construct well-organized 3DGPC frameworks. To resolve this problem, latex technology has recently been used to incorporate graphene into non-polar or highly viscous polymers, such as polypropylene (PP),65 polystyrene (PS),66 nature rubber (NR).67 As an typical example, Peng's group prepared a 3D interconnected graphene networks in NR matrix by integrating self-assembly with latex compounding technology *via* electrostatic adsorption,67 which was schematically illustrated in Figure 3d. Firstly, GO was reduced in the presence of PDDA, which renders positive charge on the graphene surface. Then the positively charged PDDA-graphene was assembled with negatively charged NR latex particles and the organization of graphene at the surface of NR latex particles was tuned by the strong electrostatic interfacial interaction between graphene and NR latex. Finally, the supernatant coagulation was processed into a composite film consisting of a 3D interconnected graphene network filled with polymer by subsequent filtering, freeze-drying and compression molding.

**Incorporating polymers into pre-synthesized 3DGFs**

Compared with the above two methods, incorporating polymers into pre-synthesized 3DGFs to produce 3DGPCs, does not require thecomplicated functionalization and dispersion of individual GO sheets, which is beneficial for overcoming any process incompatibility. With a directly conjugated graphene network infiltrated with polymers, the resulting composites typically exhibited superior electrical conductivities and mechanical properties. Not limited to reduction self-assembly of GO, CVD methods have also been used to produce the presynthesized 3DGFs with more controlled and uniform morphologies and structures. To date, several strategies including infiltration, hydrophobicity-driven absorption and electrochemical deposition have been developed for incorporating polymers into pre-synthesized 3DGFs.68-71 The highly microporous 3DGFs can allow polymers or the polymer precursors to be readily infiltrated. To avoid damaging the 3D structure when mixing 3DGFs in the polymer matrix, the vacuum-assisted infiltration technique was employed to transfer polymers or its precursor into 3D graphene networks to produce 3DGPCs. For instance, 3D rGO/EP composites were prepared by vacuum-assisted infiltration methods, which exhibited better electrical conductivity and mechanical properties than those prepared by ultrasonication-assisted solution mixing.72 Recently, taking advantage of the high oil-adsorption capacity of hydrophobic 3DGFs, a strategy to prepare 3DGPCs by hydrophobicity-driven adsorption has been developed. In this strategy, the hydrophobic 3DGFs can automatically adsorb the organic solutions of polymers in large amount. The 3DGFs, which offer a large number of accessible open pores and cell walls, can serve as the host frameworks to immobilize and support the guest polymers. For example, poly(styrene-b-(ethylene-cobutylene)-b-styrene) (SEBS), an oil-soluble commodity polymer, was selected as the functional modifiers to fabricate the 3D rGO/SEBS aerogels with the hydrophobicity-driven absorption method.68 The host 3DGFs was immersed into cyclohexane solutions containing SEBS. The $\pi$-$\pi$ interactions between the graphene sheets and the styrene segments of SEBS lead to the strong absorption of the SEBS into the 3DGFs. Thus, the hydrophobicity-driven absorption method

is expected to be a versatile route to obtain various 3DGPCs since most commodity polymers are oil-soluble. Many applications of 3DGPCs, especially electrochemistry-related applications, require the deposition of 3DGPCs on conductive substrates. However, this is usually done by firstly synthesizing 3DGPCs followed by slurry coating. Alternatively, a convenient electrochemical deposition strategy can be used to produce 3DGPC electrodes directly. Typically, using a 3D graphene foam by template-directed growth as a free-standing working electrode, Yu *et al.* prepared 3D rGO/PANI composites through a onestep electrochemical deposition process in which highly ordered polyaniline nanocone arrays were tightly attached to the surface of the 3D graphene electrode (Figure 4a).69 In

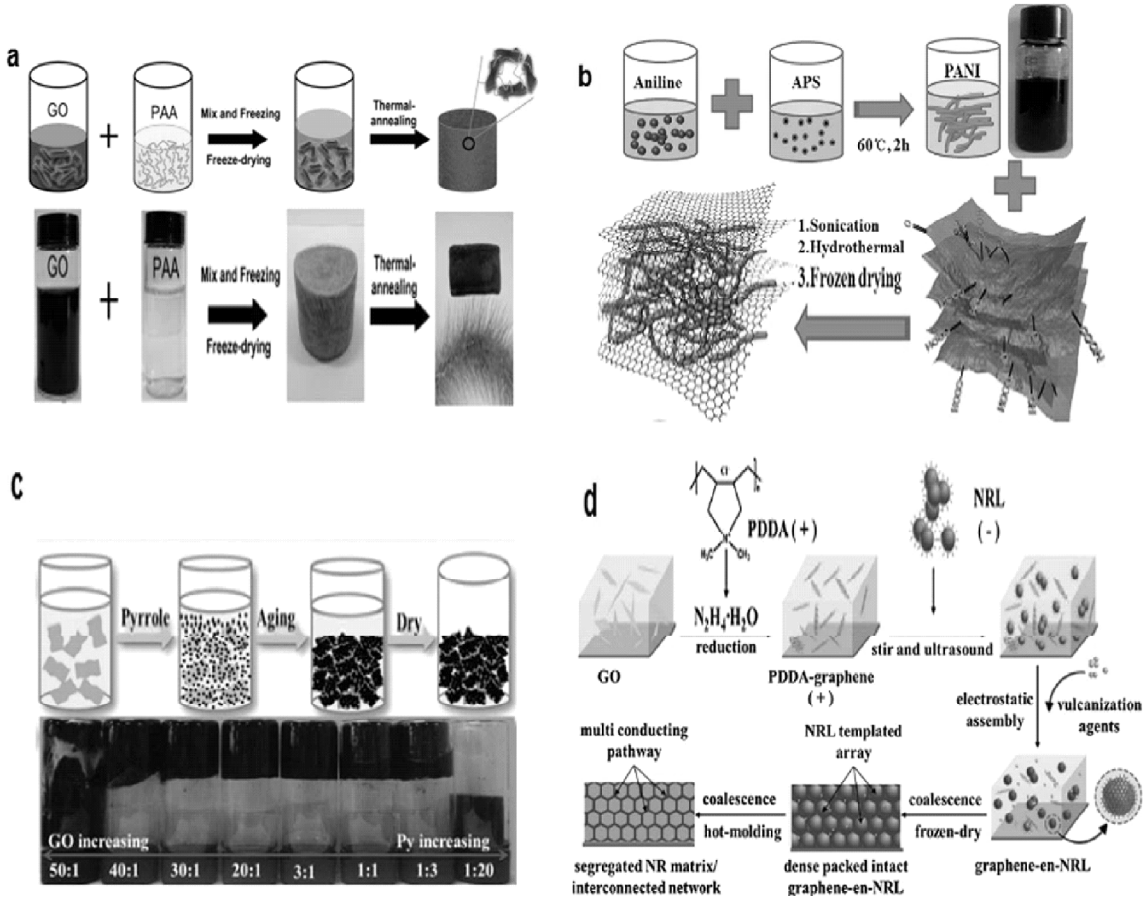


**Figure 3:** (a) Schematic illustration and digital photographs of the two-step fabrication process of 3D rGO/PI composite.Reproduced with permission from ref. 56. Copyright 2015 American Chemical Society. (b) Illustration of the process for preparation of 3D rGO/PANI hybrid aerogels. Reproduced with permission from ref. 60. Copyright 2014 Elsevier Ltd. (c) Schematic illustration of the formation mechanism of 3D rGO/PPy aerogels by one-step in situ redox reaction and the effect of the mass ratio of GO to Py on the hydrogel formation. Reproduced with permission from ref. 64. Copyright 2014 The Royal Society of Chemistry. (d) Schematic description of the multi-step process for the preparation of 3D rGO/NR composites by latex technology. Reproduced with permission from ref. 67. Copyright 2014 Elsevier Ltd.

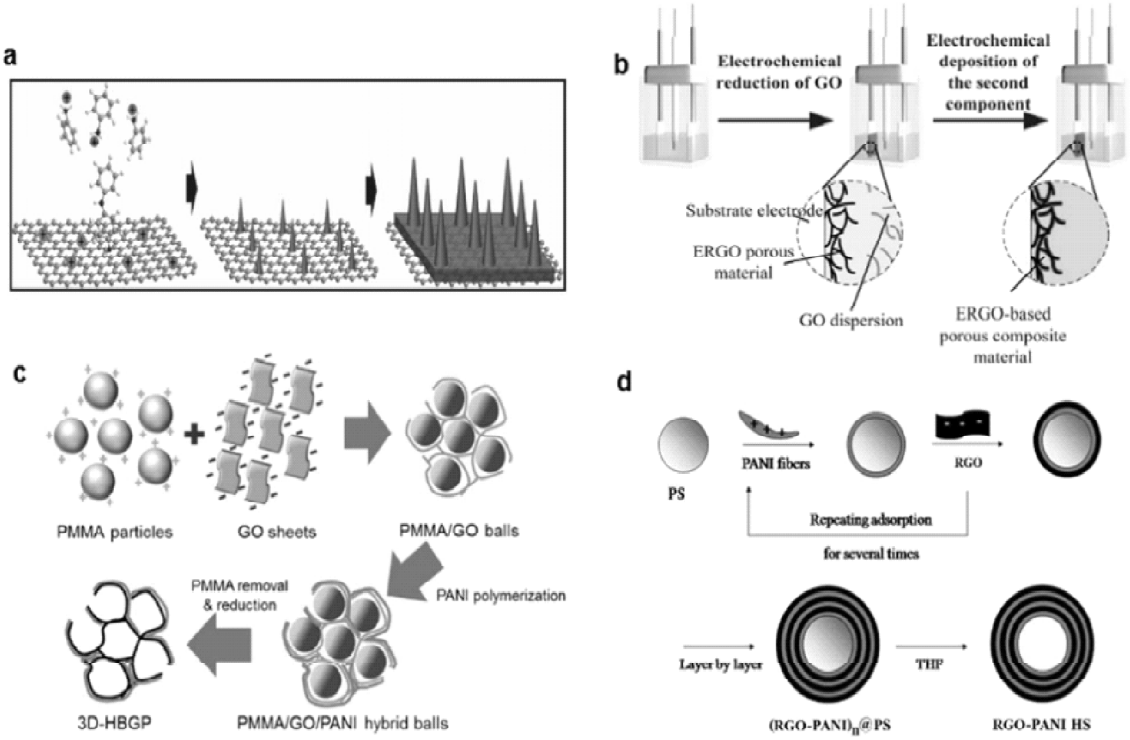


**Figure 4:** (a) One-step electrodeposition process of PANI on the surface of 3D graphene network. Reproduced with permission from ref. 69. Copyright 2015 Elsevier Ltd. (b) Schematic illustration of the two-step electrodeposition process for 3D rGO/PANI electrode. Reproduced with permission from ref. 70. Copyright 2012 The Royal Society of chemistry. (c) Schematic illustration of the fabrication of 3D rGO/PANI hybrid hollow balls using PMMA particles as template. Reproduced with permission from ref. 75. Copyright 2014 Elsevier Ltd. (d) Schematic illustration of the fabrication procedure of 3D rGO/PANI hollow sphere by layer-by layer assembly technology. Reproduced with permission from ref. 76. Copyright 2015 Elsevier Ltd.

addition, two-step consecutive electrochemical deposition process has also been used for producing 3DGPCs. Firstly, 3DGFs were grown directly on the electrode by electrochemical reduction of a concentrated GO dispersion. Subsequently, the polymers were electrochemically deposited onto this 3D rGO matrix, yielding 3DGPC materials (Figure 4b). In this way, conducting polymers, such as polyaniline (PANI) and PPy,70,71 have been successfully incorporated into 3D rGO architectures, demonstrating the versatility of this method. The prepared 3DGPC materials have a conductive graphene network as the matrix, onto which the second component is homogeneously coated. The electrochemical deposition has been proved to be an effective and green approach to produce 3DGPCs, and is attractive for electrochemical applications, since high surface area and low electrolyte transport resistance make these composites suitable for high-performance electrode materials in electrochemical devices

### Other methods

Directly mixing GO with various polymer templates, *e.g.* spongy,73 sphere,74 *et al.* is an convenient and efficient route to porous or hollow 3DGPCs. For instance, using a commercial polyurethane (PU) foam as template, 3D rGO/PU composites with interconnected porous were synthesized by self-assembly of GO sheets onto polymer skeletons, followed by the reduction of GO to rGO.73 Using polymethyl methacrylate (PMMA) colloidal particles as a template, Trung *et al.* fabricated hollow 3D rGO/PANI composite electrodes by assembling GO sheets on the surface of PMMA colloidal particles, followed by the synthesis of PANI and removal of the core PMMA particles (Figure 4c).75 Luo *et al.* designed and fabricated a 3D rGO/PANI hybrid hollow sphere *via* layer-by layer (LBL) assembly ofnegatively-charged rGO and positively charged PANI on PS microsphere, followed by the removal of the PS template (Figure 4d).76 The template method is attractive for fabricating highly ordered, mechanically flexible 3DGPCs with tunable open porous morphologies. The pore size and the number of graphene layers could be effectively controlled by the size of the templates and the GO suspension concentration or growth conditions. Recently, method of emulsion polymerization using graphene as emulsifier have also been developed for 3DGPCs. Owing to strong attraction of graphene to high-energy oil/water interfaces, waterin-oil type emulsion systems can form by utilizing graphene sheets as emulsifier (Figure 5). After polymerization of monomer in the continuous oil phase, the water-filled spherical cavities were lined with a graphitic skin consisting of overlapped graphene sheets. A gentle evaporation process removed the water, leaving an open cell composite foam with cell sizes easily tunable by varying the mixture composition. 3D graphene/PS with hollow structures have been synthesized by this environmentally friendly approach which avoids the use of chemical treatments, the input of large amounts of mechanical or thermal energy, or the addition of stabilizers such as surfactants or high boiling solvents that can be difficult to remove.77 Limitation in the choice of monomer using this approach comes from the requirement that graphene need stabilize the oil/water interface.78 The oil phase must have a lower surface energy than graphene and should be insoluble in the water phase. Since graphene and water has a surface energy of 54.8 mN m-1 and 72.9 mN m-1,79 respectively, the surface energy of the oil phase must be below 54.8 mN m-1. Thus, the low surface energy of styrene and most other monomers easily fit this criterion for producing 3DGPCs by this approach.

### Applications

Combining the excellent mechanical flexibility, high electric conductivity and large specific surface area of 3D porous graphene with the specific functions of diverse polymers, 3DGPCs can exhibit many unique or exceptional attributes in environmental protection, energy storage, sensitive detection and conducting polymer composites, *etc.*

### Environmental protection

The removal of oils and organic contaminants from water has attracted immense academic and commercial interest because of the industrial oily waste and oil spill accidents.

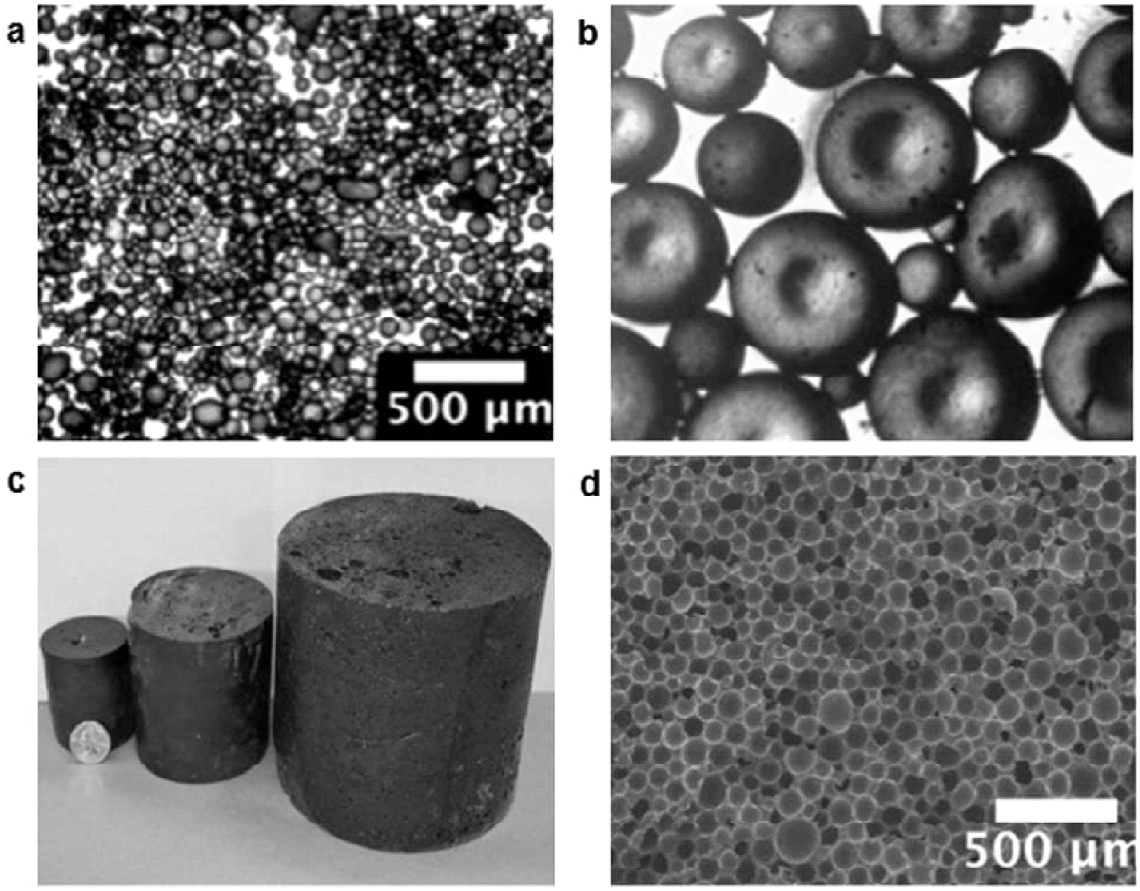


**Figure 5:** (a) Optical microscopy image of graphitic skin stabilized emulsion in 50:34:0.44 mass ratio water/heptane/graphene mixture. (b) Magnified optical microscopy image of the initial structure of the water droplets covered with graphene skin before heptane evaporation. (c) Graphene composite foams of various sizes with a US quarter for scale. (d) SEM image of a cross section of the composite after polymerization made from an emulsion with a 50:34:0.44 mass ratio water/styrene/graphene. Reproduced with permission from ref.77. Copyright 2015 American Chemical Society

Traditionally, absorption treatment is considered to be a convenient and environmentally friendly method. Due to intrinsic hydrophobicity and large specific surface area, combined with the functionality of the polymers, 3DGPCs exhibit high absorption capacity of oils and organic solvents. For example, the covalently assembled 3D rGO/PPy foams prepared by a hydrothermal method feature highly delocalizedð electrons that may readily interact with other conjugated or nonpolar molecules. 80 In particular, aromatic compounds such as benzene and toluene, π-π stacking interaction will result. For hydrocarbons such as diesel and kerosene, these nonpolar molecules can couple with the conjugated system within the 3D rGO/PPy composites *via* Van der Waals forces. Due to these interactions and pore structure, both the sorption capacities and sorption rate of 3D rGO/PPy are very high for oil (>100 g g-1) and organic solvent (>35 g g-1). However, the 3D rGO/PPy

materials absorbed not only oils but also water, which decreased the separation selectivity and efficiency. In order to absorb oil from water while repelling water completely, superhydrophobic and superoleophilic 3DGPCs, such 3D rGO/polyvinylidene (PVDF),81 3D rGO/polydimethylsiloxane (PDMS),82 have been designed and prepared. Combining the micro/nano-scale structures of graphene and low surface energy of the polymers, the as-prepared 3DGPC aerogels showed high absorption capacity of oil and organic solvents, excellent water repellency and superior absorption recyclability, and were regarded as an ideal material for removing oil and organic solvents from water. 3DGPC materials can exhibit remarkable recyclability *via* heating or squeezing. However, the heating process is relatively complicated for the recycle of the adsorbent materials, especially, when the involved solvents have a high boiling point. On the other hand, the squeezing method is generally restricted to those elastic adsorbent materials, while 3D graphene based materials generally have the disadvantages of brittle mechanical performances and are easily irreversibly damaged under mechanical deformations. Thus, it is necessary to design and construct 3D porous graphene materials with mechanical flexibility as elastic adsorbent materials in the field of oil-water separator. To this end, Jiang's group fabricated 3D rGO/polyurethane (PU) foams by self-assembly of graphene oxide sheets on commercial PU foam skeletons.73 The unique structure not only maintained the physical properties of graphene foams, but also effectively transferred load from graphene sheets to elastic PU skeletons under mechanical deformation. As a consequence, the 3D (rGO)/PU foams exhibited high hydrophobicity and excellent cycling performance. Recently, it is noticed that incorporating cross-linkable polymers into 3D rGO aerogels could greatly mitigate the delicate and fragile nature of 3D rGO aerogels.83-85 For instance, 3D rGO/cross-linkable poly(acrylic acid) (XPAA) composites with mass densities of about 4-6 mg cm -3 and >99.6% porosity can reversibly support up to 10,000 times their weight with full recovery of their original volume. 85 The average absorption capacity for six different oils (diesel, gasoline, motor oil, olive oil, pump oil and sesame oil) were measured to be around 120 g g -1 (Figure 6).

The modification of adsorbent materials with a smart surface is appealing, since the simple operation of the external stimuli could enable the removal and recovery of oil from the aqueous media. Several external stimuli could be used to trigger this adsorption and desorption process, including electricity, heating, and pH. 86,87 Among which, the pH-responsive method is most attractive because this process could rapidly reverse the adsorption and desorption process by switching the surface property between hydrophobic and hydrophilic in a short period of time. For example, Zhu *et al.* prepared the smart surface of 3D graphene foam (GF) by grafting a amphiphilic block of poly(2-vinylpyridine) and polyhexadecyl acrylate copolymer (P2VP-b-PHA) on the surface of GF. 88 The process was illustrated in Figure 7, where the GF was grafted with a block copolymer (P2VP-b-PHA) via a silanization and quaternization process. Due to the superoleophilic or superoleophobic surface at different medium pH, the as-prepared 3D composite foam could effectively absorb oil or organic solvents from the aqueous media by using its superoleophilic surface at pH of 7.0, and it could also completely release the adsorbates when the pH was switched to 3.0, with a continuous operation of many cycles (>10).

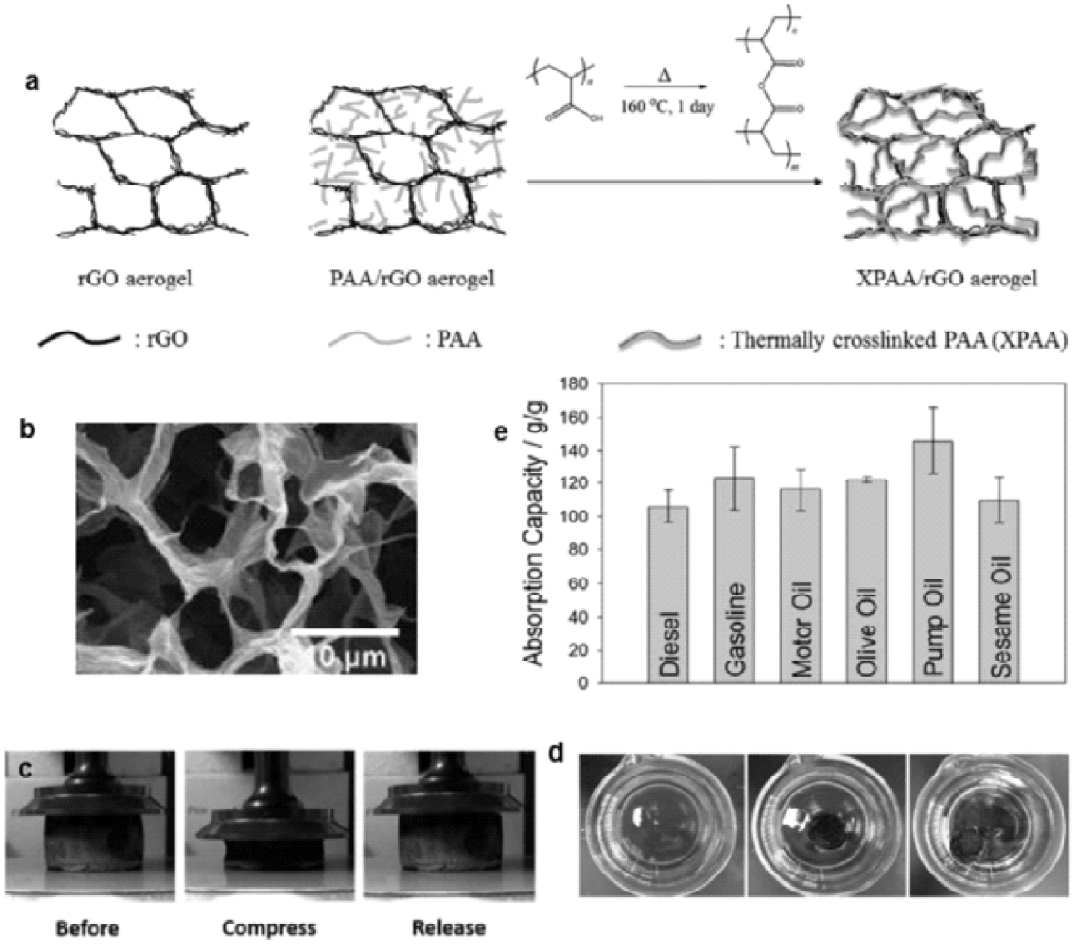


**Figure 6:** (a) Morphology of the 3D rGO/XPAA aerogels. (b) SEM images of 3D rGO/XPAA aerogels. (c) Digital images showing the compressibility of the 3D rGO/XPAA aerogels during the 10th compression/release cycle. (d) Demonstration of oil absorption using gasoline as the absorbed solvent from t=0 to t=35 s. (e) Absorption capacities for various oils expressed as gram oil per gram aerogel. Reproduced with permission from ref. 85. Copyright 2015 American Chemical Society

Furthermore, the as-prepared 3D composite foam showed superior absorption capacity for oil and organic solvent, with a high capacity of approximately 196 times its own weight.

Nowadays, the removal of the toxic molecules from industrial wastewater, especially various industrial dyes and heavy metal ions, has become a critical challenge. It is well known that GO possesses high adsorption capacities toward various water contaminants. However, the needed centrifugation after adsorption and the potential biological toxicity of GO restrict its applications in wastewater treatment. 3D GO/polymer composites possess extensive specific surface area and interconnected 3D porous network that can allow the dye molecules or heavy metal ions to diffuse easily into the adsorbent with abundant active adsorption sites. For instance, amine-functionalized 3D graphene aerogel prepared

via the interaction between GO sheets and polyethylenimine (PEI) with high amine density exhibited an extremely high adsorption capacity for acid amaranth dye (800 mg g -1 ). 89 In addition, the 3D GO/PEI also exhibited good adsorption capacity for carbon dioxide (11.2 wt % at 1.0 bar and 273 K) and formaldehyde. 90 As a kind of low-cost and effective flocculants, anionic polyacrylamide (APAM) is widely used to treat industrial and municipal wastewater. The combination of GO and APAM was suitable for practical environmental protection applications. 91 For instance, 3D GO/APAM composite gel can be used to remove basic fuchsin from aqueous solutions (Figure 8). The maximum adsorption capacity was up to 1034.3 mg g -1 . The high adsorption capacity was mainly due to the synergistic effect of the porous structure and the functional groups of the adsorbents. The cations in basic fuchsin solution easily combined with the anions in APAM by ionic bonding. The -NH 2 groups of basic fuchsin also easily interacted with the polar group of APAM by hydrogen bonding and intermolecular force. There may be π-π interactions between basic fuchsin and GO caused by some double bonds. Recently, biopolymers such as DNA, chitosan (CHI), amylopectin, bovine serum albumin (BSA), etc. have been used to mediate GO gels. 92 The prepared 3D composite gels could act as

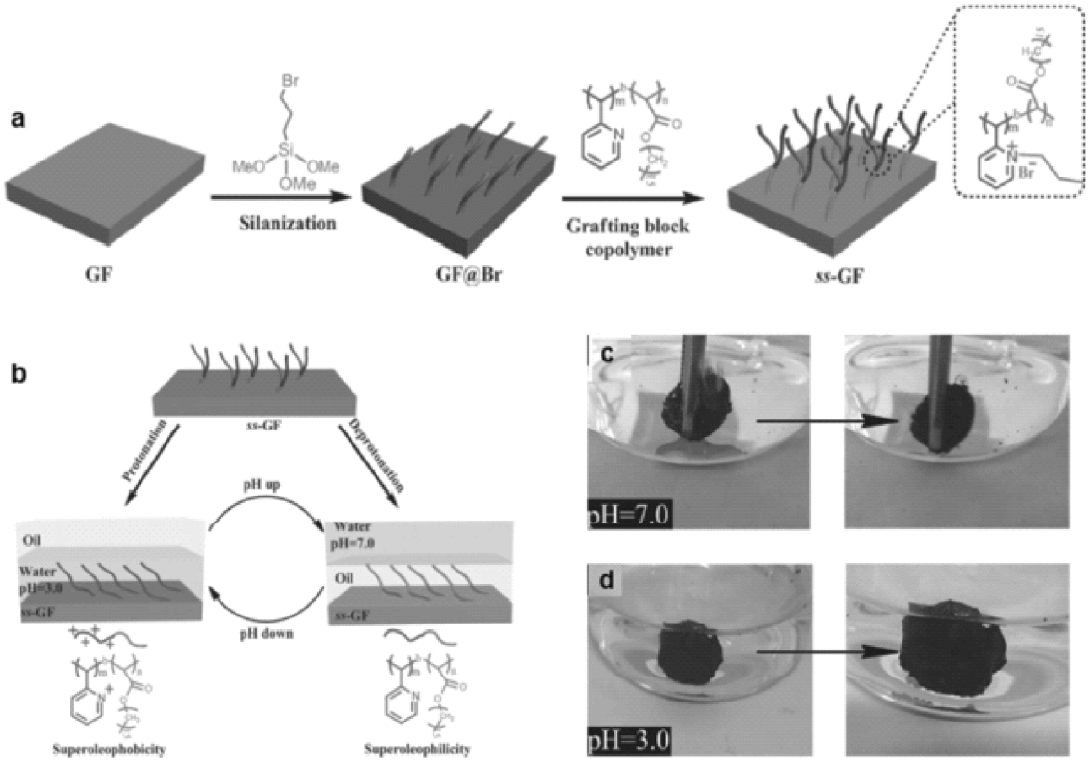


**Figure 7:** (a) Schematic illustration of the process to fabricate 3DGPC with smart surface (ss-GF). (b) Schematic illustration of switchable wettability of the as-fabricated ss-GF. (c) The adsorption of chloroform by the ss-GF in water of pH 7.0. (d) The desorption of chloroform by the ss-GF in water of pH 3.0. Reproduced with permission from ref. 88. Copyright 2015 WILEY-VCH Verlag GmbH & Co. KGaA, Weinheim.

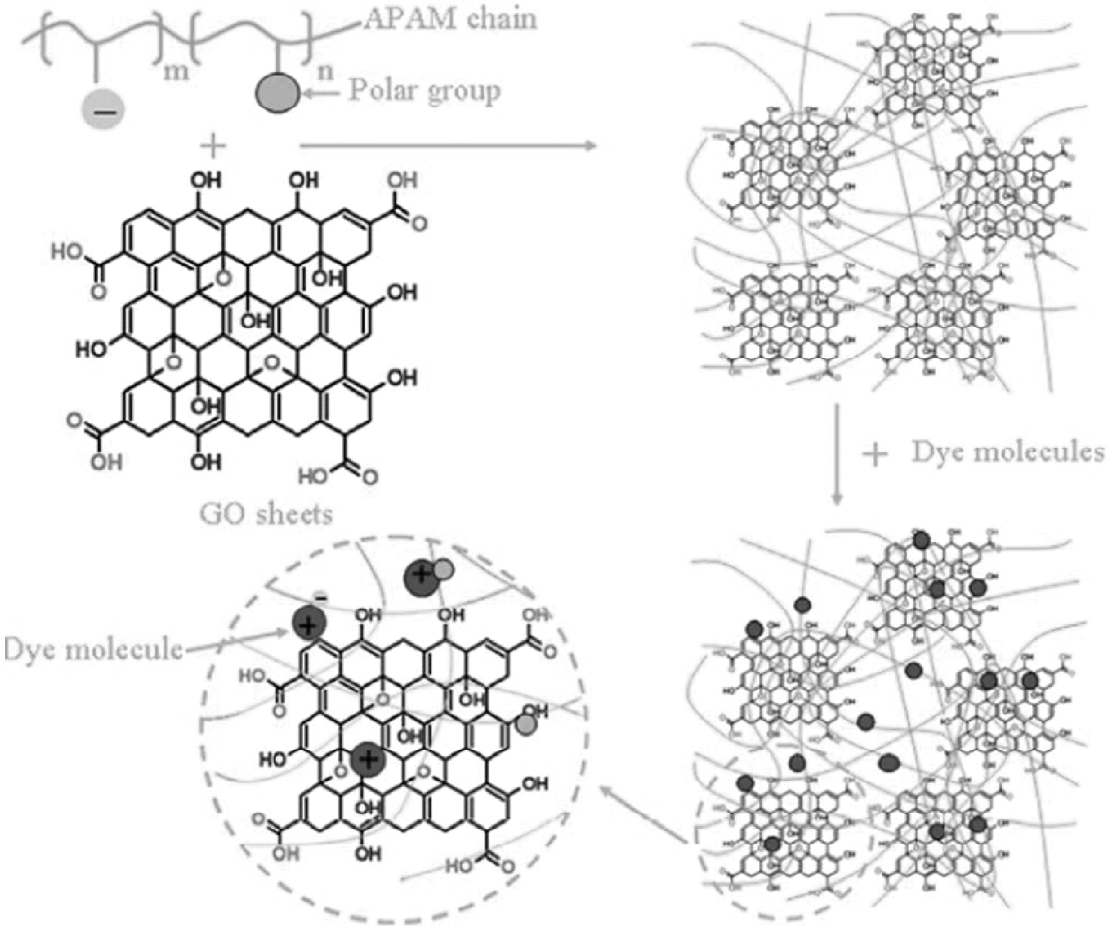


**Figure 8:** The schematic of the combination of APAM, GO and basic fuchsin molecules. Combining charge neutralization and excellent bridging cohesion, APAM molecular chain is immobilized on the surface of GO to form stable composites. Basic fuchsin molecules easily go through the loose holes into the internal network and bond with APAM or GO by ionic interaction, hydrogen bonding, and intermolecular force. Reproduced with permission from ref. 91. Copyright 2015 Elsevier Inc.

promising adsorbents for removal of industrial dyes and heavy metal ions in wastewater. On one hand, well-defined and interconnected 3D porous framework of 3D GO/ biopolymer gels allowed the adsorbate molecules to diffuse easily into the adsorbent. On the other hand, when GO was decorated by hydrophilic biopolymers, the original amphiphilic surface of GO became too hydrophilic to interact with or partition into lipid bilayers. Thus, its cell toxicity could be greatly suppressed and the biological compatibility was improved. For example, Cheng et al. designed and fabricated three typical 3D GO/ biopolymers (BSA, CS and DNA) hydrogels to remove cationic dyes and heavy metal ions from wastewater. 93 The adsorption capacity was as high as 1100 mg g -1 for methylene blue (MB) dye and 1350 mg g -1 methyl violet (MV) dye. In addition, the GO/biopolymer

gels also exhibited high adsorption capacity on heavy metal ions. The maximum adsorption capacities of GO/BSA, GO/CS, and GO/DNA for Pb 2+ were 110, 129, and 147 mg g -1 respectively; and the adsorption amounts for Cu 2+ were 391, 370, and 480 mg g -1 , respectively. The strong adsorption capacity of the 3D GO/biopolymers gels possibly resulted from the synergistic effects of the static electric attraction and the surface complexation between the hydroxyl/amino groups and heavy metal ions. Other examples, 3D GO/DNA hydrogel exhibited a total dye-loading capacity of 960 mg g -1 for safranine O., which was comparable to many carbon nanomaterials (210-785 mg g -1 for the ordered mesoporous carbon). 46 A hydrophilic and biocompatible 3D rGO/CHI mesostructures with large specific surface area (603.2 m 2 g -1 ) could achieve a removal efficiency of 97.5% for reactive black 5 (RB5) at a concentration of 1.0 mg mL -1 . 94 Wang et al. fabricated magnetic 3D GO/CHI composites combining the features of the high surface area of GO and abundant amino and hydroxyl functional groups of CHI, which were utilized to immobilize Candida rugosa lipase via different routes and showed excellent immobilization capacities. 95 Zhang et al. prepared a 3D rGO/amylopectin (AP) through the hydrogen-bonding interaction between AP and GO in the presence of hydrazine hydrate acting as a reducing reagent. 96 The obtained 3D rGO/AP framework exhibited excellent adsorption performance toward hemoglobin in the presence of other protein species. It provided a maximum adsorption capacity of 1,010 mg g -1 and an adsorption efficiency of 92.7%. Electromagnetic radiation has become a pollution problem, which is harmful to both highly sensitive precision electronic equipment and the health of human beings. Therefore, electromagnetic absorption materials have attracted considerable attention and the electromagnetic absorption properties of various nanostructures have been widely investigated. To date, electromagnetic absorption materials with strong absorption abilities and lightweight characteristics have been greatly desired. 3D graphene structures have some unique characteristics such as low density, high porosity, large specific surface area and good electrical conductivity. Hence, 3D graphene networks are promising candidates for the construction of lightweight electromagnetic wave absorbing materials. 97 However, because of the high conductivity, graphene has a strong dielectric loss but a weak attenuation to electromagnetic waves. It is found that the deposition of other dielectric nanostructures on the surface of the graphene sheets is an efficient way to fabricate lightweight materials for strong electromagnetic absorbents. 98,99 For instance, as PANI nanorod arrays were grown on the surface of graphene sheets, the electromagnetic absorption properties of the materials were significantly enhanced. 100 The maximum reflection loss reached -45.1 dB for 3D G/PANI nanorod arrays with a thickness of only 2.5 mm. The absorption bandwidth with the reflection loss below -20 dB was up to 10.6 GHz as its thickness was in the range of 2-4 mm. The enhanced electromagnetic absorption properties were attributed to the improved dielectric relaxation, the special structural characteristics and the charge transfer from PANI nanorods to graphene sheets. Moreover, the amount of the material added into the paraffin matrix was only 20 wt%. Thus, the 3D G/PANI nanorod arrays are very promising as lightweight electromagnetic absorbing materials. In another case, Wu et al. prepared a 3D rGO/Poly (3,4-ethylenedioxythiophene) (PEDOT) composites as electromagnetic absorption materials. 101 The electromagnetic

absorption properties were tested by uniformly mixing 10 wt% of 3D rGO/PEDOT with a paraffin matrix under coaxial wire analysis. Apparent absorbing ranges deeper than -10 dB under different thicknesses were observed in Figure 9. When the sample thickness reached 2 mm, it showed not only the maximum absorption value (-35.5 dB), but also the widest bandwidth from 11.5 to 16.5GHz with a reflection loss deeper than -10 dB. These results indicate that the 3D rGO/PEDOT possesses good electromagnetic absorption capabilities in both low- and high-frequency bands under different thicknesses with a low content ratio of 3D rGO/PEDOT in the composite.

## Energy storage

Supercapacitors, known as an important class of electrochemical energy storage device, has attracted intense interest over past decades, owing to its high power density, long cycle life, and high rate capability. 102 Based on the energy storage mechanism, supercapacitors store charges using either ion adsorption at the interface of electrode and electrolyte (electric double-layer capacitors, EDLCs) or fast surface redox reactions (pseudocapacitors). Recently, 3D graphene macrostructures have emerged one of most promising electrode materials for EDLCs, due to the highly interconnected pore structure, fast ion and mass transfer, highly percolated electronic transport, low density, and exceptionally large surface area and easy access to surface adsorption sites. 103-105 On the other hand, conducting polymers, especially PANI and PPy, that exhibit much higher theoretical capacitance than carbon materials, have been used as electrode materials for pseudocapacitors due to their superior redox properties and easy synthesis. However, their poor cycling stability limits the practical application owing to the swelling and shrinkage during the charge/discharge process. 106 Incorporation the pseudocapacitive

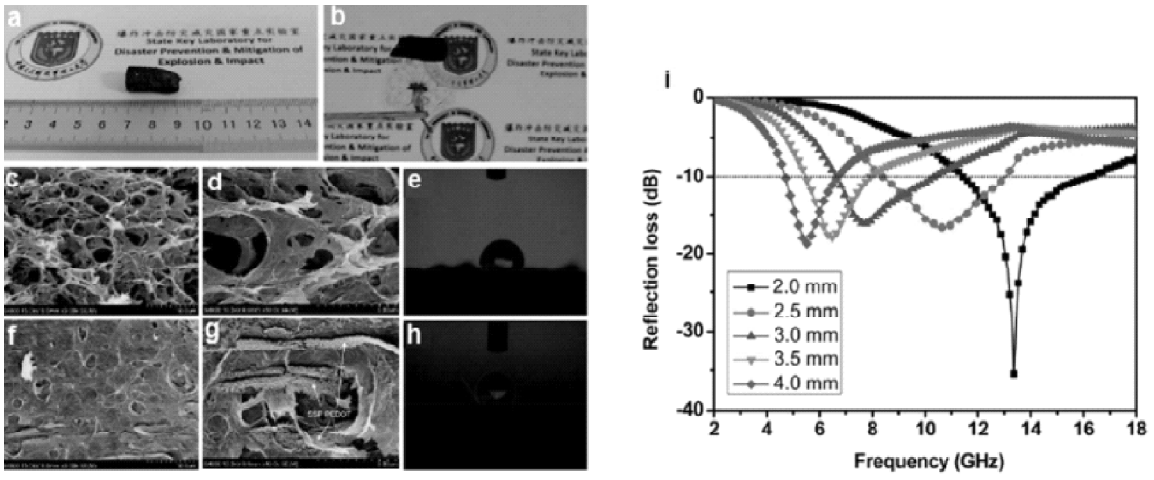


**Figure 9:** (a and b) Optical image of 3D rGO. (c and d) SEM images of 3D rGO. (e) Contact angle of 3D rGO (113.5°). (f and g) SEM images of 3D rGO/PEDOT. (h) Contact angle of 3D rGO/PEDOT (123.4°). (i) Reflection loss curves for samples of 3D rGO/PEDOT with different thickness (2.0 to 4.0 mm) in the frequency range of 2-18 GHz. Reproduced with permission from ref. 101. Copyright 2014. The Royal Society of Chemistry

materials into the 3D graphene macrostructures has the potential to take advantage of both components to enable greatly improved overall performance. Generally, the 3D graphene/conducting polymer composites could be prepared by in situ chemical polymerization or electropolymerization of monomer in the presence of 3DGFs, or directly mixing the solutions of polymers and GO and then assembling both components through an in situ reduction process. 107-110 The incorporation of nanostructured polymers, such as nanowires, nanorods, nanotubes, nanocones, in the electrode material can enhance the accessibility of electrolyte ions to the surface of active materials and reduce the ions diffusion distance during electrochemical charge/discharge process. 69,111,112 For example, 3D graphene network coated with vertically aligned PANI nanocones can deliver a high specific capacitance of 751.3F g -1 in 1 M HClO 4 at a current density of 1.0 A g -1 , with 93.2% of initial capacitance remained after 1000 charging/discharging cycles. 69 Hollow micro/nanostructured materials have been recognized as one type of promising materials with numerous applications in energy-related fields. Design and construction of 3DGPCs with hollow nanostructure can greatly enlarge the specific surface area, providing highly electroactive regions and short diffusion lengths for both charge and ion transport. 74, 113-114 For instance, Fan *et al.* fabricated the graphene/PANI hollow spheres by wrapping graphene oxide on a polyaniline hollow sphere via electrostatic interaction followed by electrochemical reduction of GO. 74 The wrapping of rGO sheets on the PANI hollow spheres can offer highly conductive pathways by bridging individual PANI hollow spheres together, thus greatly improve the rate and cycling performance of supercapacitors. The specific capacitance of 3D rGO/PANI hybrids can reach 614 F g -1 at a current density of 1 A g -1, and retain 90% after 500 charging/discharging cycles at a current density of 1 A g -1, indicating a good cycling stability. The lack of intrinsic electrochemical activity for 3D graphene foams (GF) prepared by a CVD method with metal foams as templates, limits their capacitive performance. The macro-sized pores (around several hundreds of micrometres) are efficient to facilitate electrolyte transfer but do not contribute to the areal capacitance. 115 Nevertheless, the 3D GF provides an excellent platform with high electric conductivity and porosity on which conducting polymers can be deposited for various electrochemical applications. The shortcoming of electrodepositing polymers on 3DGFs is that only a thin layer of conducting polymers has been coated on the surface of graphene, resulting in small areal capacitance. Thus, it is highly desirable to fill the macro-sized pores with pseudocapacitive materials with smaller pores in order to boost its areal capacitance. To this end, Chan-Park's group constructed a bicontinuous macroporous graphene foam composed of few-layered graphene sheets, 116 and used it as a highly conductive platform to grow mesoporous polyaniline via electrodeposition and inkjet techniques. The preparation procedure was illustrated in Figure 10 (a-b). PANI thin film was first coated on 3DGF by a galvanostatic electropolymerization method at a current density of 2 mA cm -2 . Then, aniline monomers were inkjet printed into the pores of the PANI-coated graphene foam and subsequently oxidative polymerized to produce porous PANI hydrogel with the help of phytic acid. The coating PANI thin layer on the surface of 3DGF via electrodeposition is of importance for changing the hydrophobic surface to a hydrophilic one and for the subsequent filling

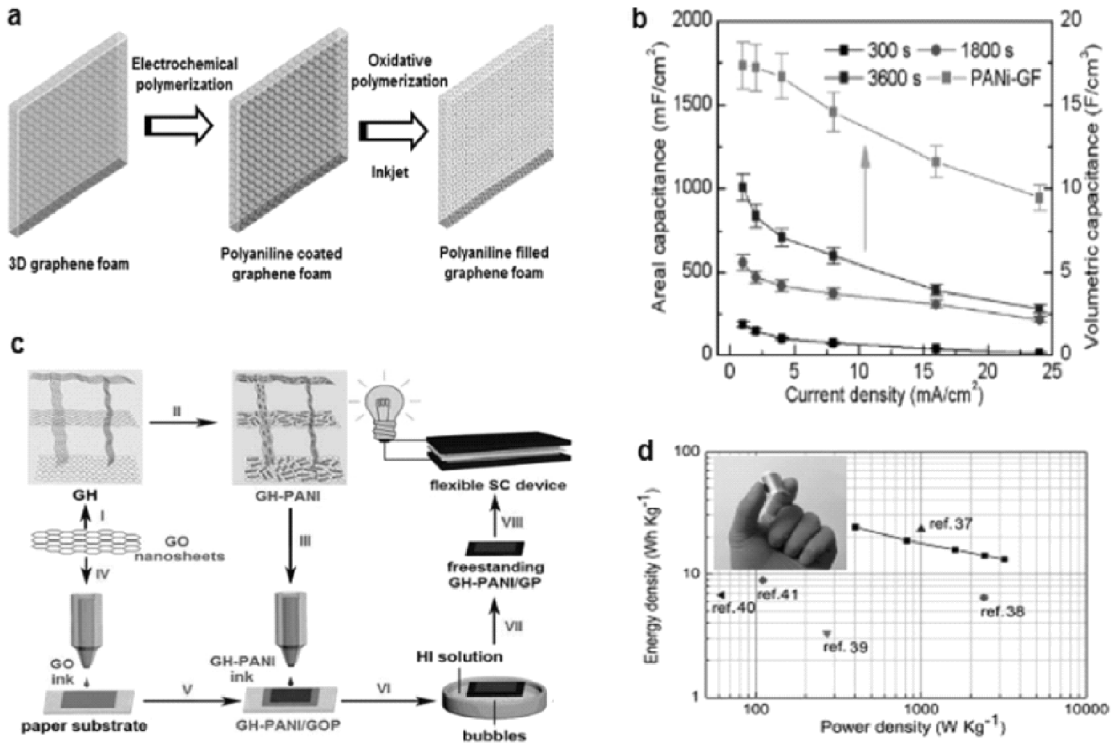


**Figure 10:** (a) Illustration of the preparation procedure of PANI-filled 3DGF via electrodeposition and inkjet techniques. (b) Areal capacitances of PNAI-coated 3DGF foam with different deposition times and PANI-filled 3DGF foam. Reproduced with permission from ref. 116. Copyright 2014 American Chemical Society. (c) Schematic illustration of the fabrication process of 3D rGO/PANI/GP. (d) Ragone plots of the SC device compared with data in other literature. Reproduced with permission from ref. 119. Copyright 2014 American Chemical Society

of the mesoporous PANI network into the macroporous graphene foam. When used as electrode materials for supercapacitors, the 3D graphene/PANI network with high porosity renders a large areal capacitance of over 1700 mF cm -2, which is over two times enhancement in comparison with the pure graphene foam and PANI thin layer coated one. The ultrahigh areal capacitance benefits from the synergistic effect of the good conductive graphene backbone and highly pseudocapacitive PANI nanostructure. Flexible, light-weight and wearable supercapacitors have attracted significant attention in energy storage because of their potential application in portable electronic devices, flexible displays, electronic papers and mobile phones. 117 The free-standing and binder-free electrode with robust mechanical strength and large capacitance is a vital factor for flexible supercapacitors. For instance, Zhang's group fabricated a symmetric flexible supercapacitor using free-standing 3D rGO/PANI foams as both electrodes. 118 Owing to the well-ordered porous structure and high electrochemical performance of the 3D rGO/PANI composites, the symmetric device in 1 M $H_2SO_4$ electrolyte exhibited a specific capacitance of 790 F g -1 , a maximum energy density and power density of 17.6 W h kg -1 and 98 kW kg -1 .

Moreover, the device possessed an excellent cycle life with an 80% capacitance retention after 5000 cycles. Chi et al. developed a flexible all-solid-state supercapacitor with two pieces of high-performance binder-free nanohybrid graphene paper (GP) electrode using $PVA/H_3PO_4$ as the gel electrolyte. 119 The paper electrode was fabricated based on fully inkjet printing synthesis of a freestanding GP supported 3D rGO/PANI nanocomposite. The preparation procedure was illustrated in Figure 10 (c-d). The flexible all- solid-state supercapacitor exhibited remarkable mechanical flexibility, high cycling performance and impressive energy density of 24 Wh kg -1 at a power density of 400 W kg -1. Capacitive deionization (CDI), an electrosorption process that involves forcing an ionic species toward oppositely charged electrodes with large surface area under an electric field, is considered as a very energy efficient water desalination technology. 120 With their unique structural characteristics and chemical tuanibility, 3DGPCs represent a promising electrode material for the design of high- performance CDI devices. As an example, Gu et al. prepared 3D rGO/PPy composite electrodes by a two- step hydrothermal process, including in situ polymerization of PPy and then reduction of GO in the presence of KMnO4. 61 The resulting 3D rGO/PPy composite electrodes exhibited a hierarchical porous structure with a specific surface area of 331 m 2 g -1 and excellent specific capacity of 356 F g -1 . The enhanced electrochemical capacity and low inner resistance enables 3D rGO/PPy composite electrodes with an outstanding specific electrosorptive capacity of 18.4 mg g -1, demonstrating the exciting potential of 3D rGO/PPy electrodes for high-performance and low energy consumption capacitive deionization. Furthermore, the 3D rGO/PPy composite electrodes could be regenerated by a simple short circuit without additional driving energy and secondary pollution, which is beneficial for large scale application. 3D graphene/conducting polymer composites have been used as electrodes not only in supercapacitors, but also in biological or chemical batteries. Typically, 3D graphene/PNAI foams can be used as anodes in microbial fuel cell (MFC). 121 The electrode was prepared by in situ depositing PANI on the 3DGF foams obtained by CVD method. The 3D G/ PNAI foam can allow high bacterial biofilm loading and ensure the efficient extracellular electron transfer, and thus function as MFC anode with remarkable performance. In another case, 3D graphene/conducting polymers composites have also explored as cathode materials for various chemical batteries, harnessing the high electrical conductivity of graphene and the redox capability of conducting polymers. For instance, Li et al. developed a high- performance 3D rGO/PPy cathode material for implantable, biocompatible zinc/ polymer batteries utilizing biofluids as the electrolyte. 122 The long and tangled PPy fibers were evenly distributed on the rGO nanosheets which were coated with a sheer layer of the amorphous PPy. The large-scale two- dimensional coated graphene sheets decorated with fine PPy fibers possessed a larger specific surfaces area than the PPy fibers. Not surprisingly, the specific surface area and the conductivity of the composite were significantly increased to 561 $m^2g^{-1}$ and 141 $Scm^{-1}$, respectively. Both the large surface area and high electrical conductivity were crucial for a cathode material to ensure high electrochemical catalytic activity. The battery constructed with 3D rGO/PPy cathode and Zn anode can deliver an energy density of 264 mWh g -1 in 0.1 M phosphate-buffer saline. Recently, Shen *et al.* designed and fabricated a category of 3D rGO/PANI/$LiFePO_4$

composites for cathode materials of lithium-ion batteries through in situ redox reaction of GO and aniline in the aqueous suspension of $LiFePO_4$. 63 The as-prepared 3D rGO/PANI composites were intertwined and coated uniformly on the surface of $LiFePO_4$. Comparably, the 3D rGO/PANI/$LiFePO_4$ composites exhibited larger reversible specific capacity, superior rate capability, and excellent cycling stability, when compared with the bare $LiFePO_4$ or the $LiFePO_4$ modified with 3D graphene or PANI alone.

**Sensitive detection**

Recently, 3DGPCs were explored as electrochemical detection sensors, and exhibited superior sensing performance due to its porous microstructure and strong and selective adsorption of the target ions or molecules. 123,124 For instance, Wang et al. developed a 3D rGO/Ppy electrode for the electrochemical detection of Hg2+ in aqueous solution, which exhibited high sensitivity and selectivity. 74 The mechanism of this sensing process was believed to be that Hg 2+ ions can selectively coordinate with the nitrogen atoms of the pyrrole units of PPy. 125 The limit of detection was measured to be as low as 0.03 nM (30 ppt), which was much lower than the guideline value of 2 ppb for drinking water given by the World Health Organization. Recently, Yang et al. used 3D rGO/PANI as the sensitive layer of a DNA adsorbent for detecting Hg 2+ . 126 Amino-group-rich 3D rGO/ PANI exhibited high affinity toward the immobilization of T-rich DNA strands, which prefer to bind with Hg 2+ to form T-Hg 2+ -T coordination (Figure 11). The results demonstrated that the electrochemical biosensor based on 3D rGO/PANI nanocomposite showed high sensitivity and selectivity toward Hg 2+ within a concentration range from 0.1 nM to 100 nM with a low detection limit of 0.035 nM. Yang et al. prepared interconnected 3D GO/SPAN (a copolymer of aniline and m-aminobenzenesulfonic acid) composite electrode through dripping the GO/SPAN mixture solution on the carbon paste electrode (CPE) surface and then drying naturally in the air. 127 Because the negative charge and specific structure of the nanocomposite can prompt the adsorption of positively charged guanine and adenine via strong π-π interactions or electrostatic adsorption, the 3D GO/ SPAN hybrid was adopted as an excellent sensing platform for highly sensitive determination of guanine and adenine. Biological modification of monolithic and porous 3D graphene is of great significance for extending its application for highly sensitive biosensors. For example, by one-step electrochemical depositing CHI on the free-standing 3D graphene electrode, a 3D graphene/CHI enzymatic biosensor was created for glucose detection with a large linear range (5.0 μM to 19.8 mM in the phosphate buffer solution), a low detection limit (1.2 μM), and a rapid response (reaching the 95% steady-state response within 8 s). 128 Tan's group presented a hierarchical porous chitosan/vacuum-stripped graphene/ polypyrrole (CHI/VSG/PPy) scaffold as a free-standing and flexible electrochemical sensor for dopamine detection. 129 The CHI/VSG/PPy composite electrode was fabricated via a two-step strategy involving freeze-casting and electrochemical polymerization techniques, and exhibited good selectivity, high sensitivity (632.1 μA mM -1 cm -2 ), wide linear response range (0.1-200 μM), low detection limit (19.4 nM, S/N = 3) and good sensing performance in human serum samples, which is highly comparable with the Au modified electrode. 130

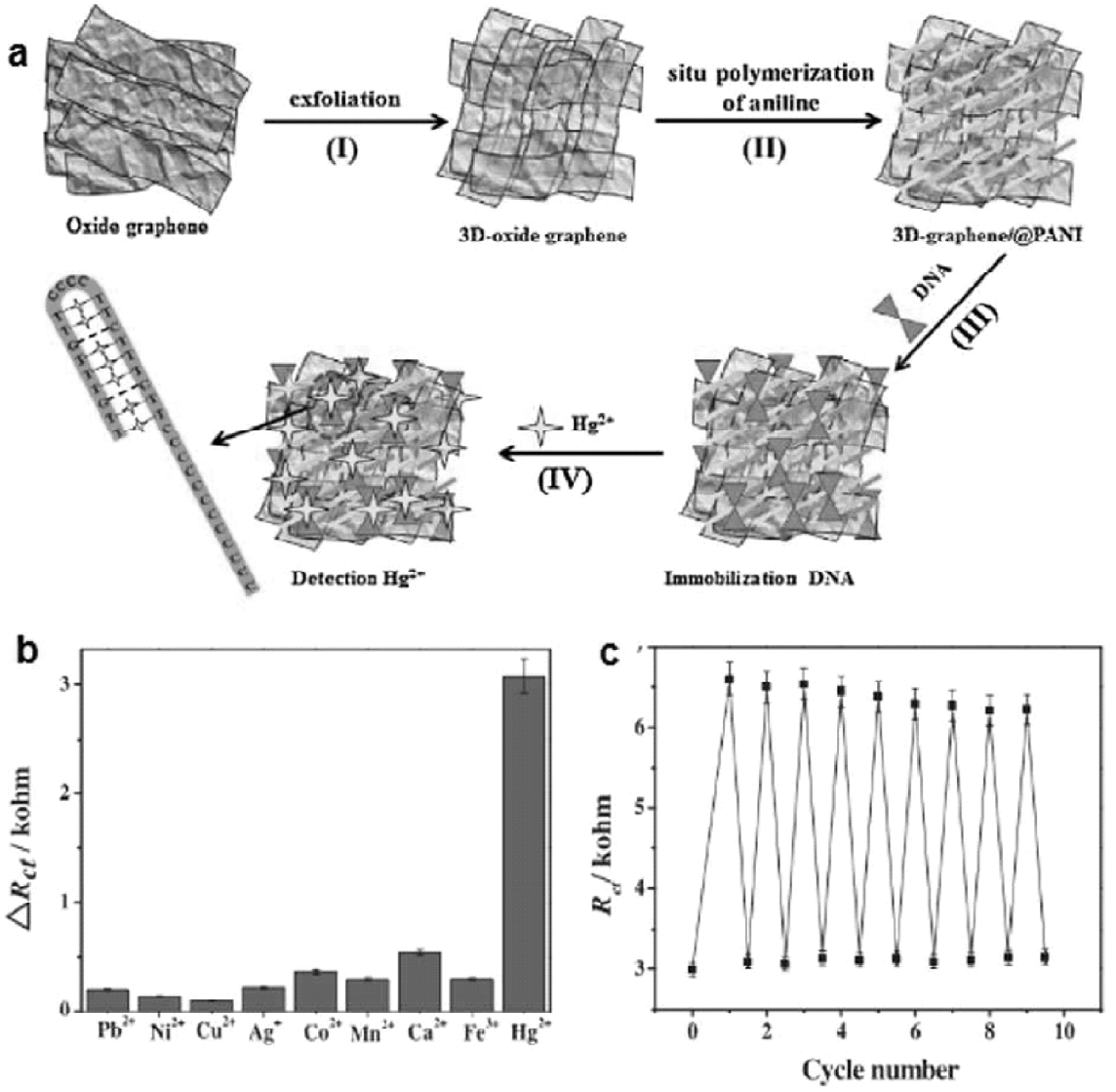


**Figure 11:** (a) Schematic illustration of the detection of Hg 2+ ions using the DNA biosensor based on 3D rGO/PANI composite. (b) R ct change in the presence of 10 μM of other metal ions and 0.1μM Hg 2+ ions. (c) Reusability of EIS-based Hg 2+ sensor challenged with 100 nM Hg 2+ ions and washed with 50 mM cysteine. Reproduced with permission from ref. 126. Copyright 2015 Elsevier Ltd.

## Conducting polymer composites

Constructing an infinite connected network of conducting fillers in an insulating polymer matrix is important to improve the electrical conductivity of composites. By using ultralight 3DGFs as a unique integrated graphene filler rather than dispersing rGO into the matrix, aggregation or segregation of rGO can be prevented such that the effective conductive pathway could form at a relatively low loading. At present, the most widely used method

to produce 3DGFs is self- assembly by reduction of exfoliated GO. 131,132 For instance, Fan et al. developed firstly a 3D rGO/poly (methyl methacrylate) (PMMA) composites by backfilling PMMA into the pores of the 3DGFs, providing uniform distribution of interconnected few-layer rGO sheets in the PMMA matrix. 133 As graphene loadings increased from 0.67 to 2.50 vol.%, the 3D rGO/PMMA composites exhibited significant increases in electrical conductivity (0.160-0.859 S m -1) and thermal conductivity (0.35-0.70 W/m K) compared with those of pure PMMA as well as the rGO/PMMA composites prepared by traditional dispersion methods. Interestingly, 3D rGO/epoxy (EP) composites with exceptional anisotropic structure have also been prepared by infiltrating 3D rGO with EP resin (Figure 12). 134 The unusual structure of the composites gave rise to 67% and 113% higher electrical conductivity and fracture toughness, respectively, in the alignment direction than those in the transverse. However, two drawbacks limited the application of 3D rGO in conductive composites: structural defects and easy agglomeration in the matrix. 135-137 Fortunately, graphene grown by the CVD method possesses intact structure and higher conductivity, which makes it an attractive candidate for application in conductive composites. For instance, Chen et al. fabricated 3D graphene/PDMS composites by infiltrating PDMS into CVD grown 3D graphene foam. [137] Introduction of the PDMS matrix did not damage the interconnected scaffold of 3DGFs, because the electrical conductivity of 3DGFs showed nearly no change after infiltration with PDMS. Thus, the prepared 3D G/PDMS composites showed a very high electrical conductivity of ~10 S cm -1 at an ultralow graphene loading of ~0.22 vol.%. This value was ~6 orders of magnitude higher than that of chemically derived graphene-based composites, indicating significant advantages of 3DGFs in the use of composites for electrical applications. Nevertheless, the residues and unstable doping which are common for CVD graphene, may deteriorate its properties. When PEDOT:PSS was introduced into CVD graphene, it works as both supporting layer and dopant, and thus these two problems get resolved favorably. Therefore, the combination of CVD graphene and PEDOT:PSS would produce composites with better electrical properties. When the content of graphene and PEDOT:PSS were 1.5 wt% and 1.5 wt% respectively, the 3D composite showed a very high electrical conductivity (24 S cm -1), which was ~1.6 times higher than CVD graphene/PDMS (3 wt% graphene loading, 15 S cm -1) prepared as a reference. 138 3D rGO/polymer conducting composites can be used as a sensing device for differentiating organic solvents with different polarity. Such a device operates on a basis of swelling effect. Organic solvents cause the polymer to swell, which reduces the number of electrical conduction paths through the composite material, leading to an increase in the overall resistance of the composite material. For instance, Zhang *et al.* prepared the 3D graphene/PDMS conducting composite by infiltrating PDMS into the 3D graphene network. 139 PDMS can swell in response to various organic solvents and the degree of its swelling is related to the polarity of the solvents, with the swelling degree increasing with decreasing solvent polarity. The 3D graphene/polymer conducting composites can also be utilized as a strain sensor with high sensitivity, which can find important applications in real-time monitoring of buildings, such as a bridge, dam, and high-speed railway. For instance, Xu et al. prepared a double-layer 3D GF/PDMS- poly(ethylene terephthalate) (PET) composite by infiltrating

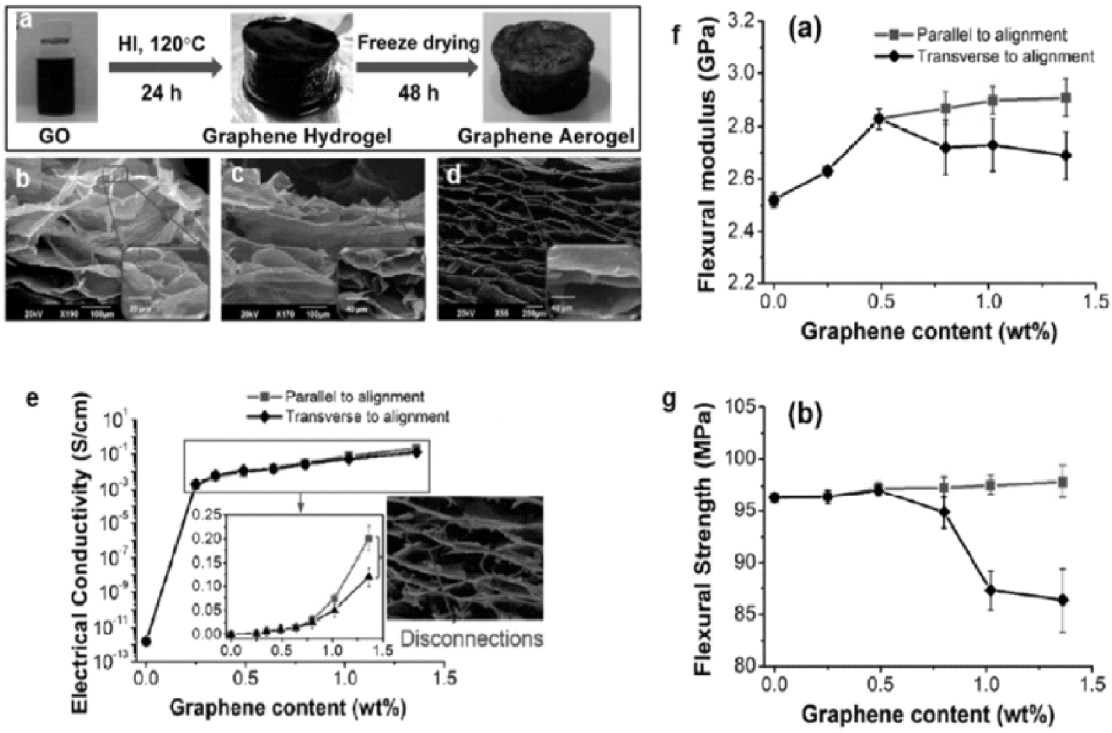


**Figure 12:** (a) Schematic illustration of the fabrication process of 3D rGO and SEM images of 3D rGO prepared using GO dispersions at different concentrations of (b) 0.5, (c) 1.5, and (d) 2.0 mg mL -1 . (e) Electrical conductivity of 3D rGO/EP composites in the direction parallel to the alignment and transverse to it. (f) Flexural modulus and (g) strength of 3D rGO/EP composites. Reproduced with permission from ref. 134. Copyright 2015 American Chemical Society.

PDMS into 3D GF, and then introducing a thin layer of PET as substrate to improve the bending sensitivity of 3D GF/PDMS. 140 The resistance of the 3D GF/PDMS-PET composite was increased when bended to the side of PET, whereas its resistance would be decreased when bended to the side of GF. For both cases, the absolute value of the relative variation of electrical resistance was increased with the bending curvature. More importantly, the relative variation of electrical resistance for double-layer 3D GF/PDMS-PET composite could be up to six times higher than single-layer 3D GF/PDMS composite for the same bending curvature. These observations made 3D GF/PDMS-PET well suitable as a strain sensor.

## Conclusions and Perpectives

In summary, considerable efforts have recently been exerted to the design and fabrication of various 3DGPCs, to explore both the fundamental bottom-up synthetic chemistry and their potential applications in environmental protection, energy storage, sensitive detection and conducting composites (Table 1). Compared with other 3D graphene based composites, such as 3D G/metal oxide, 3D G/CNT, research in 3DGPCs remains at its initial stage. The rapid growth of this field assures us that 3DGPCs will be a generation of versatile

materials for various purposes. With more synthetic strategies being developed, a wide range of advanced 3DGPCs with elaborated structures, chemical functionalities and physical properties can be readily prepared. Beyond the exciting progress to date, we believe that there are considerable challenges and opportunities remaining for continued investigation. Firstly, the fundamental 3D self-assembly chemistry between graphene as a 2D macromolecule and various polymers need to be further studied for developing more synthetic strategies and 3DGPCs. Secondly, the intrinsic microstructures within the 3DGPCs including the distribution of polymers and the interfaces of graphene and polymers are partly unclear and need to be further clarified to achieve a deep understanding of the structure-property relationship for efficiently tailoring the materials' performance by design. Thirdly, more functional polymers can be rationally introduced into the 3DGFs to further expand the functions and applications of 3DGPCs. So far, multifunctional 3DGPCs that simultaneously exhibit strechability, flexibility, compressibility and self-repair property have not been realized but are highly desired for smart and wearable electronic products. Moreover, 3DGPCs with diverse morphologies such as single phase interpenetrating double-network, bicontinuous structure, et al. are desirable for many applications areas particularly in electrochemical devices that require both efficient transport of electrons and ions. For example, recently, a 3D bicontinuous nanotubular graphene/PPy composite has been developed by electrodepositing PPy on CVD synthesized nanotubular graphene, which has been used as free standing supercapacitor electrodes with high specific capacitance of 509 F g -1, excellent cycle stability and outstanding rate performance. 141 Finally, large-scale and low-cost fabrication of 3DGPCs is a critical issue for their practical widespread applications. With the multidisciplinary efforts from chemistry, physics, biology, and materials science, as well as a combination of many unique attributes, we believe that 3DGPCs could open up significant technological opportunities in diverse areas in the near future.

## *References*

[1] Novoselov, K. S.; Geim, A. K.; Morozov, S. V.; Jiang, D.; Zhang, Y.; Dubonos, S. V.; Grigorieva, I. V.; Firsov, A. A. Electric Field Effect in Atomically Thin Carbon Films. Science 2004, 306, 666-669.

[2] Weiss, N. O.; Zhou, H.; Liao, L.; Liu, Y.; Jiang, S.; Huang, Y.; Duan, X. Graphene: An Emerging Electronic Materials. Adv. Mater. 2012, 24, 5782-5825.

[3] Novoselov, K. S.; Fal'ko, V. I.; Colombo, L.; Gellert, P. R.; Schwab, M. G.; Kim, K. A Roadmap for Graphene. Nature 2012, 490, 192-200.

[4] Shao, Y.; EI-Kady, M. F.; Wang, L. J.; Zhang, H.; Li, Y.; Wang, H.; Mousavi, M. F.; Kaner, R. B. Graphene-Based Materials for Flexible Supercapacitors. Chem. Soc. Rev., 2015, 44, 3639-3665.

[5] Huang, X.; Zeng, Z.; Fan, Z.; Liu, J.; Zhang, H. Graphene-Based Electrodes. Adv. Mater. 2012, 24, 5979-6004.

[6] Papandrea, B.; Xu, X.; Xu, Y.; Chen, C.-Y.; Lin, Z.; Wang, G.; Luo, Y.; Liu, M.; Huang, Y.; Mai, L.; Duan, X. Three-Dimensional Graphene Framework with Ultra-High Sulfur Content for a Robust LithiumSulfur Battery. Nano Res. 2016, 9, 240-248.

[7] Bi, H.; Xie, X.; Yin, K.; Zhou, Y.; Wan, S.; He, L.; Xu, F.; Banhart, F.; Sun, L.; Ruoff, R. S. Spongy Graphene As a Highly Efficient and Recyclable Sorbent for Oils and Organic Solvents. Adv. Funct. Mater. 2012, 22, 4421-4425.

[8] Xu, Y.; Chen, C.-Y.; Zhao, Z.; Lin, Z.; Lee, C.; Xu, X.; Wang, C.; Huang, Y.; Shakir, M. I.; Duan, X. Solution Processable Holey Graphene Oxide and Its Derived Macrostructures for High-Performance Supercapacitors. Nano Lett. 2015, 15, 4605-4610.

[9] Hu, H.; Zhao, Z.; Wan, W.; Gogotsi, Y.; Qiu, J. Ultralight and Highly Compressible Graphene Aerogels. Adv. Mater. 2013, 25, 2219-2223.

[10] Cao, X.; Shi, Y.; Shi, W.; Lu, G.; Huang, X.; Yan, Q.; Zhang, Q.; Zhang, H. Preparation of Novel 3D Graphene Networks for Supercapacitor Applications. Small 2011, 7, 3163-3168.

[11] Yavari, F.; Chen, Z.; Thomas, A. V.; Ren, W.; Cheng, H.-M.; Koratkar, N. Macroscopic ThreeDimensional Graphene Foam Network. Sci. Rep. 2011, 1, 166.

[12] Fan, D.; Liu, Y.; He, J.; Zhou, Y.; Yang, Y. Porous Graphene-Based Materials by Thermolytic Cracking. J. Mater. Chem. 2012, 22, 1396-1402.

[13] Zhang, X.; Ziemer, K. S.; Zhang, K.; Ramirez, D.; Li, L.; Wang, S.; Hope-Weeks, L. J.; Weeks, B. L. Large-Area Preparation of High-Quality and Uniform Three-Dimensional Graphene Networks Through Thermal Degradation of Graphene Oxide–Nitrocellulose Composites. ACS Appl. Mater. Interfaces 2015, 7, 1057-1064.

[14] Liu, W.; Li, H.; Zeng, Q.; Duan, H.; Guo, Y.; Liu. X.; Sun, C.; Liu, H. Fabrication of Ultralight Three-Dimensional Graphene Networks with Strong Electromagnetic Wave Absorption Properties. J. Mater. Chem. A 2015, 3, 3739-3747.

[15] Xue, M.; Chen, D.; Wang, X.; Chen, J.; Chen, G. F. Carbonized Poly(vinylidene fluoride)/Graphene Oxide with Three-Dimensional Multiscale-Pore Architecture As an Advanced Electrode Material. J. Mater. Chem. A 2015, 3, 7715-7718.

[16] Peng, Q.; Li, Y.; He, X.; Gui, X.; Shang, Y.; Wang, C.; Wang, C.; Zhao, W.; Du, S.; Shi, E.; Li, P.; Wu, D.; Cao, A. Graphene Nanoribbon Aerogels Unzipped from Carbon Nanotube Sponges. Adv. Mater. 2014, 26, 3241-3247.

[17] Zhang, Y.; Zhen, Z.; Zhang, Z.; Lao, J.; Wei, J.; Wang, K.; Kang, F.; Zhu, H. In-situ Synthesis of Carbon Nanotube/Graphene Composite Sponge and Its Application As Compressible Supercapacitor Electrode. Electrochim. Acta 2015, 157, 134-141.

[18] Zhang, R.; Cao, Y.; Li, P.; Zang, X.; Sun, P.; Wang, K.; Zhong, M.; Wei, J.; Wu, D.; Kang, F.; Zhu, H. Three-Dimensional Porous Graphene Sponges Assembled with the Combination of Surfactant and Freeze-Drying. Nano Res., 2014, 7, 1477-1487.

[19] Huang, M.; Pascal, T. A.; Kim, H.; Goddard, W. A.; Greer, J. R. Electronic-Mechanical Coupling in Graphene from in situ Nanoindentation Experiments and Multiscale Atomistic Simulations. Nano Lett. 2011, 11 , 1241-1246.

[20] Wang, L. J.; EI-Kady, M. F.; Dubin, S.; Hwang, J. Y.; Shao, Y; Marsh, K.; McVerry, B.; Kowal, M. D.; Mousavi, M. F.; Kaner, R. B. Flash Converted Graphene for Ultra-High Power Supercapacitors. Adv. Energy Mater. 2015, 5, 1500786.

[21] Luo, B.; Zhi, L. Design and Construction of Three Dimensional Graphene-Based Composites for Lithium Ion Battery Applications. Energ. Environ. Sci. 2015, 8, 456-477.

[22] Yu. M.; Huang, Y.; Li, C.; Zeng, Y.; Wang, W.; Li, Y.; Fang, P.; Lu, X.; Tong, Y. Building ThreeDimensional Graphene Frameworks for Energy Storage and Catalysis. Adv. Funct. Mater. 2015, 25, 324-330.

[23] Chen, K.; Li, C.; Chen, Z.; Shi, L.; Reddy, S.; Meng, H.; Ji, Q.; Zhang, Y.; Liu, Z. Bioinspired Synthesis of CVD Graphene Flakes and Graphene-Supported Molybdenum Sulfide Catalysts for Hydrogen Evolution Reaction. Nano Res., 2016, 9, 249-259.

[24] Gonçalves, G. A. B.; Pires, S. M. G.; Simões, M. M. Q.; Neves, M. G. P. M. S.; Marques, P. A. A. P. Three-Dimensional Graphene Oxide: a Promising Green and Sustainable Catalyst for Oxidation Reactions at Room Temperature. Chem. Commun. 2014, 50, 7673-7676.

[25] Yang, G.; Lee, C.; Kim, J. Three-Dimensional Graphene Network-Based Chemical Sensors on Paper Substrate. J. Electrochem. Soc. 2013, 160, B160-B163.

[26] Nardecchia, S.; Carriazo, D.; Ferrer, M. L.; Gutiérrez, M. C.; Monte, F. Three Dimensional Macroporous Architectures and Aerogels Built of Carbon Nanotubes and/or Graphene: Synthesis and Applications. Chem. Soc. Rev. 2013, 42, 794-830.

[27] Liu, F.; Piao, Y.; Choi, J. S.; Seo, T. S. Three-Dimensional Graphene Micropillar Based Electrochemical Sensor for Phenol Detection. Biosens. Bioelectron 2013, 50, 387-392.

[28] Ni, Y.; Chen, L.; Teng, K.; Shi, J.; Qian, X.; Xu, Z.; Tian, X.; Hu, C.; Ma, M. Superior Mechanical Properties of Epoxy Composites Reinforced by 3D Interconnected Graphene Skeleton. ACS Appl. Mater. Interfaces 2015, 7, 11583-11591.

[29] Longo, S.; Mauro, M.; Daniel, C.; Musto, P. Guerra, G. Rayleigh Scattering by Graphene-Oxide in Syndiotactic Polystyrene Aerogels. Carbon 2014, 77, 896-905.

[30] Yang, T.; Zhang, H.; Wang, Y.; Li, X.; Wang, K.; Wei, J.; Wu, D.;Li, Z.; Zhu, H. Interconnected Graphene/ Polymer Micro-Tube Piping Composites for Liquid Sensing. Nano Res., 2014, 7, 869-876.

[31] Yang, J.; Zhang, E.; Li, X.; Zhang, Y.; Qu, J.; Yu, Z.-Z. Cellulose/Graphene Aerogel SupportedPhase Change Composites with High Thermal Conductivity and Good Shape Stability for Thermal Energy Storage. Carbon 2016, 98, 50-57.

[32] Shaeli lessa, K. H.; Zhang, Y.; Zhang, G.; Xiao, F.; Wang, S. Conductive Porous Sponge-Like Ionic Liquid-Graphene Assembly Decorated with Nanosized Polyaniline As Active Electrode Material for Supercapacitor. J. Power Sources 2016, 302, 92-97.

[33] Zhu.; Teng, K.; Shi, J.; Chen, L.; Xu, Z. A Facile Assembly of 3D Robust Double Network Graphene/ Polyacrylamide Architectures via γ-Ray Irradiation. Compos. Sci. Technol. 2016, 123, 276-285.

[34] Xu, Y.; Sheng, K.; Li, C.; Shi, G. Self-Assembled Graphene Hydrogel via a One-Step Hydrothermal Process. ACS Nano 2010, 4, 4324-4330.

[35] Xu, Y.; Shi, G.; Duan, X. Self-Assembled Three-Dimensional Graphene Macrostructures: Synthesis and Applications in Supercapacitors. Accounts Chem. Res. 2015, 48, 1666-1675.

[36] Li, D.; Müller, M. B.; Gilje, S.; Kaner, R. B.; Wallace, G. G. Processable Aqueous Dispersions of Graphene Nanosheets. Nat. Nanotechnol. 2008, 3, 101-105.

[37] Huang, L.; Li, C.; Yuan, W.; Shi, G. Strong Composite Films with Layered Structures Prepared by Casting Silk Fibroin-Graphene Oxide Hydrogels. Nanoscale 2013, 5, 3780-3786.

[38] Ye, S.; Feng, J.; Wu, P. Highly Elastic Graphene Oxide-Epoxy Composite Aerogels via Simple Freeze-Drying and Subsequent Routine Curing. J. Mater. Chem. A 2013, 1, 3495-3502.

[39] Wan, W.; Li, L.; Zhao, Z.; Hu, H.; Hao, X.; Winkler, D. A.; Xi, L.; Hughes, T. C.; Qiu, J. Ultrafast Fabrication of Covalently Cross-Linked Multifunctional Graphene Oxide Monoliths. Adv. Funct. Mater. 2014, 24, 4915-4921.

[40] Ji, X.; Cui, L.; Xu, Y.; Liu, J. Non-Covalent Interactions for Synthesis of New Graphene Based Composites. Compos. Sci. Technol. 2015, 106, 25-31.

[41] Bai, H.; Li, C.;Wang, X.; Shi, G. A pH-Sensitive Graphene Oxide Composite Hydrogel. Chem. Commun. 2010, 46, 2376-2378.

[42] Vickery, J. L.; Patil, A. J.; Mann, S. Fabrication of Graphene-Polymer Nanocomposites With HighOrder Three-Dimensional Architectures. Adv. Mater. 2009, 21, 2180-2184.

[43] Tao, Y.; Kong, D.; Zhang, C.; Lv, W.; Wang, M.; Li, B.; Huang, Z.-H.; Kang, F.; Yang, Q.-H. Monolithic Carbons with Spheroidal and Hierarchical Pores Produced by the Linkage of Functionalized Graphene Sheets. Carbon 2014, 69, 169-177.

[44] Bai, H.; Li, C.; Wang, X.; Shi, G. On the Gelation of Graphene Oxide. J. Phys. Chem. C 2011, 115, 5545-5551.

[45] Li, C.; Shi, G. Functional Gels Based on Chemically Modified Graphenes. Adv. Mater. 2014, 26, 3992-4012.

[46] Xu, Y.; Wu, Q.; Sun, Y.; Bai, H.; Shi, G. Three-Dimensional Self-Assembly of Graphene Oxide and DNA into Multifunctional Hydrogels. ACS Nano 2010, 4, 7358-7362.

[47] Chen, Y.; Qi, Y.; Yan, X.; Ma, H.; Chen, J.; Liu, B.; Xue, Q. Green Fabrication of Porous Chitosan/ Graphene Oxide Composite Xerogels for Drug Delivery. J. Appl. Polym. Sci. 2014, 131, 596- 602.

[48] Ouyang, W.; Sun, J.; Memon, J.; Wang, C.; Geng, J.; Huang, Y. Scalable Preparation of ThreeDimensional Porous Structures of Reduced Graphene Oxide/Cellulose Composites and Their Application in Supercapacitors. Carbon 2013, 62, 501-509.

[49] Wan, Y.; Chen, X.; Xiong, G.; Guo, R.; Luo, H. Synthesis and Characterization of ThreeDimensional Porous Graphene Oxide/Sodium Alginate Scaffolds with Enhanced Mechanical Properties. Mater. Express 2014, 4, 429-434.

[50] Guo, W.; Wang, S.; Yu, X.; Qiu, J.; Li, J.; Tang, W.; Li, Z.; Mou, X.; Liu, H.; Wang, Z. Construction of a 3D rGO-Collagen Hybrid Scaffold for Enhancement of the Neural Differentiation of Mesenchymal Stem Cells. Nanoscale 2016, 8, 1897-1904.

[51] Xu, Y.; Lin, Z.; Zhong, X.; Huang, X.; Weiss, N. O.; Huang, Y.; Duan, X. Holey Graphene Frameworks for Highly Efficient Capacitive Energy Storage. Nat. Commun. 2014, 5, 4554-4561.

[52] Xu, Y.; Lin, Z.; Zhang, X.; Papandrea, B.; Huang, Y.; Duan, X. Solvated Graphene Frameworks As High-Performance Anodes for Lithium-Ion Batteries. Angew. Chem. Int. Ed. 2015, 54, 5345-5440.

[53] Zhao, Y.; Hu, C.; Hu, Y.; Cheng, H.; Shi, G.; Qu, L. A Versatile, Ultralight, Nitrogen-Doped Graphene Framework. Angew. Chem. Int. Ed. 2012, 51, 11371-11375.

[54] Xu, Y.; Lin, Z.; Huang, X.; Liu, Y.; Huang, Y.; Duan, X. Flexible Solid-State Supercapacitors Based on Three-Dimensional Graphene Hydrogel Films. ACS Nano 2013, 7, 4042-4049.

[55] Xu, Y.; Lin, Z.; Huang, X.; Wang, Y.; Huang, Y.; Duan, X. Functionalized Graphene HydrogelBased High-Performance Supercapacitors. Adv. Mater. 2013, 25, 5779-5784.

[56] Qin, Y.; Peng, Q.; Ding, Y.; Lin, Z.; Wang, C.; Li, Y.; Xu, F.; Li, J.; Yuan, Y.; He, X.; Li, Y. Lightweight, Super-elastic, and Mechanically Flexible Graphene/Polyimide Nanocomposite Foam for Strain Sensor Application. ACS Nano 2015, 9, 8933-8941.

[57] Hu, N.; Zhang, L.; Yang, C.; Zhao, J.; Yang, Z.; Wei. H.; Liao, H.; Feng, Z.; Fisher, A.; Zhang, Y.; Xu, Z. J. Three-Dimensional Skeleton Networks of Graphene Wrapped Polyaniline Nanofibers: an Excellent Structure for High-Performance Flexible Solid-State Supercapacitors. Sci. Rep. 2016, 6, 19777.

[58] Liu, X.; Shang, P.; Zhang, Y.; Wang, X.; Fan, Z.; Wang, B.; Zheng, Y. Three-Dimensional and Stable Polyaniline-Grafted Graphene Hybrid Materials for Supercapacitor Electrodes. J. Mater. Chem. A 2014, 2, 15273-15278.

[59] Ye, S.; Feng, J. Self-Assembled Three-Dimensional Hierarchical Graphene/Polypyrrole Nanotube Hybrid Aerogel and Its Application for Supercapacitors. ACS Appl. Mater. Interfaces 2014, 6, 9671-9679.

[60] Yang, F.; Xu, M.; Bao, S.; Wei, H.; Chai, H. Self-Assembled Hierarchical Graphene/Polyaniline Hybrid Aerogels for Electrochemical Capacitive Energy Storage. Electrochim. Acta 2014, 137, 381-387.

[61] Gu, X.; Yang, Y.; Hu, Y.; Hu, M.; Huang, J.; Wang, C. Facile Fabrication of Graphene–Polypyrrole– Mn Composites As High-Performance Electrodes for Capacitive Deionization. J. Mater.Chem. A 2015, 3, 5866-5874.

[62] Zhou, Q.; Li, Y.; Huang, L.; Li, C.; Shi, G. Three-Dimensional Porous Graphene/Polyaniline Composites for High-Rate Electrochemical Capacitors. J. Mater. Chem. A 2014, 2, 17489-17494.

[63] Shen, W.; Wang, Y.; Yan, J.; Wu, H.; Guo, S. Enhanced Electrochemical Performance of Lithium Iron(II) Phosphate Modified Cooperatively via Chemically Reduced Graphene Oxide and Polyaniline. Electrochim. Acta 2015, 173, 310-315.

[64] Sun, R.; Chen, H.; Li, Q.; Song, Q.; Zhang, X. Spontaneous Assembly of Strong and Conductive Graphene/Polypyrrole Hybrid Aerogels for Energy Storage. Nanoscale 2014, 6, 12912-12920.

[65] Fu, S.; Li, N.; Wang, K.; Zhang, Q.; Fu, Q. Reduction of Graphene Oxide with the Presence of Polypropylene Micro-Latex for Facile Preparation of Polypropylene/Graphene Nanosheet Composites. Colloid Polym. Sci. 2015, 293, 1495-1503.

[66] Zhao, P.; Luo, Y.; Yang, J.; He, D.; Kong, L.; Zheng, P.; Yang, Q. Electrically Conductive Graphene-Filled Polymer Composites with Well Organized Three-Dimensional Microstructure. Mater. Lett. 2014, 121, 74-77.

[67] Luo, Y.; Zhao, P.; Yang, Q.; He, D.; Kong, L.; Peng, Z. Fabrication of Conductive Elastic Nanocomposites via Framing Intact Interconnected Graphene Networks. Compos. Sci. Technol. 2014, 100, 143-151.

[68] Ye, S.; Feng, J. Towards Three-Dimensional, Multi-Functional Graphene-Based Nanocomposite Aerogels by Hydrophobicity-Driven Absorption. J. Mater. Chem. A 2014, 2, 10365-10369.

[69] Yu, M.; Ma, Y.; Liu, J.; Li, S. Polyaniline Nanocone Arrays Synthesized on Three-Dimensional Graphene Network by Electrodeposition for Supercapacitor Electrodes. Carbon 2015, 87, 98-105.

[70] Chen, K.; Chen, L.; Chen, Y.; Bai, H.; Li, L. Three-Dimensional Porous Graphene-Based Composite Materials: Electrochemical Synthesis and Application. J. Mater. Chem. 2012, 22, 20968-20976.

[71] Wang, M.; Yuan, W; Yu, X.; Shi, G. Picomolar Detection of Mercury (II) Using a ThreeDimensional Porous Graphene/Polypyrrole Composite Electrode. Anal. Bioanal. Chem. 2014, 406, 6953-6956.

[72] Tang, G.; Jiang, Z.-G.; Li, X.; Zhang, H.-B.; Dasari, A.; Yu, Z.-Z. Three Dimensional Graphene Aerogels and Their Electrically Conductive Composites. Carbon 2014, 77, 592-599.

[73] Wu, C.; Huang, H.; Wu, X.; Qian, R.; Jiang, P. Mechanically Flexible and Multifunctional Polymer-Based Graphene Foams for Elastic Conductors and Oil-Water Separators. Adv. Mater. 2013, 25, 5658-5662.

[74] Fan, W.; Zhang, C.; Tjiu, W. W.; Pramoda, K. P.; He, C.; Liu, T. Graphene-Wrapped Polyaniline Hollow Spheres As Novel Hybrid Electrode Materials for Supercapacitor Applications. ACS Appl. Mater. Interfaces 2013, 5, 3382-3391.

[75] Trung, N. B.; Tam, T. V.; Kim, H. R.; Hur, S. H.; Kim, E. J.; Choi, W. M. Three-Dimensional Hollow Balls of Graphene-Polyaniline Hybrids for Supercapacitor Application. Chem. Eng, J. 2014, 255, 89-96.

[76] Luo, J.; Ma, Q.; Gu, H.; Zheng, Y.; Liu, X. Three-Dimensional Graphene-Polyaniline Hybrid Hollow Spheres by Layer-by-Layer Assembly for Application in Supercapacitor. Electrochim. Acta 2015, 173, 184-192.

[77] Woltornist, S. J.; Carrillo, J.-M. Y.; Xu, T. O.; Dobrynin, A. V.; Adamson, D. H. Polymer/Pristine Graphene Based Composites: From Emulsions to Strong, Electrically Conducting Foams. Macromolecules 2015, 48, 687-693.

[78] Woltornist, S. J.; Oyer, A. J.; Carrillo, J.-M. Y.; Dobrynin, A. V.; Adamson, D. H. Conductive Thin Films of Pristine Graphene by Solvent Interface Trapping. ACS Nano 2013, 7, 7062-7066.

[79] Coleman, J. N. Liquid-Phase Exfoliation of Nanotubes and Graphene. Adv. Funct. Mater. 2009, 19, 3680-3695.

[80] Li, H.; Liu, L.; Yang, F. Covalent Assembly of 3D Graphene/Polypyrrole Foams for Oil Spill Cleanup. J. Mater. Chem. A 2013, 1, 3446-3453.

[81] Li, R.; Chen, C.; Li, J.; Xu, L.; Xiao, G.; Yan, D. A Facile Approach to Superhydrophobic and Superoleophilic Graphene/Polymer Aerogels. J. Mater. Chem. A 2014, 2, 3057-3064.

[82] Hu, H.; Zhao, Z.; Wan, W.; Gogotsi, Y.; Qiu, J. Polymer/Graphene Hybrid Aerogel with High Compressibility, Conductivity, and "Sticky" Superhydrophobicity. ACS Appl. Mater. Interfaces 2014, 6, 3242-3249.

[83] Hong, J.-Y.; Bak, B. M.; Wie, J. J.; Kong, J.; Park, H. S. Reversibly Compressible, Highly Elastic, and Durable Graphene Aerogels for Energy Storage Devices under Limiting Conditions. Adv. Funct. Mater. 2015, 25, 1053-1062.

[84] Sun, H.; Xu, Z.; Gao, C. Multifunctional, Ultra-Flyweight, Synergistically Assembled Carbon Aerogels. Adv. Mater. 2013, 25, 2554-2560.

[85] Ha, H.; Shanmuganathan, K.; Ellison, C. J. Mechanically Stable Thermally Crosslinked Poly(acrylic acid)/Reduced Graphene Oxide Aerogels. ACS Appl. Mater. Interfaces 2015, 7, 6220-6229.

[86] Sun, S.; Wu, P. A One-Step Strategy for Thermal- and pH-Responsive Graphene Oxide Interpenetrating Polymer Hydrogel Networks. J. Mater. Chem. 2011, 21, 4095-4097.

[87] Zhu, C.-H.; Lu, Y.; Peng, J.; Chen, J.-F.; Yu, S.-H. Photothermally Sensitive Poly(Nisopropylacrylamide)/ Graphene Oxide Nanocomposite Hydrogels As Remote Light-Controlled Liquid Microvalves. Adv. Funct. Mater. 2012, 22, 4017-4022.

[88] Zhu, H.; Chen, D.; Li, N.; Xu, Q.; Li, H.; He, J.; Lu, J. Graphene Foam with Switchable Oil Wettability for Oil and Organic Solvents Recovery. Adv. Funct. Mater. 2015, 25, 597-605.

[89] Liang, J.; Cai, Z.; Li, L.; Guo, L.; Geng. J. Scalable and Facile Preparation of Graphene Aerogel for Air Purification. RSC Adv. 2014, 4, 4843-4847.

[90] Sui,Z.-Y.; Cui, Y.; Zhu, J.-H.; Han, B.-H. Preparation of Three-Dimensional Graphene Oxide–Polyethylenimine Porous Materials As Dye and Gas Adsorbents. ACS Appl. Mater. Interfaces 2013, 5,9172-9179.

[91] Yang, X.; Li, Y.; Du, Q.; Sun, J.; Chen, L.; Hu, S.; Wang, Z.; Xia, Y.; Xia, L. Highly Effective Removal of Basic Fuchsin from Aqueous Solutions by Anionic Polyacrylamide/Graphene Oxide Aerogels. J. Colloid Interf. Sci. 2015, 453, 107-114.

[92] Javadi, A.; Zheng, Q.; Payen, F.; Javadi, A.; Altin, Y.; Cai, Z.; Sabo, R.; Gong, S. Polyvinyl Alcohol-Cellulose Nanofibrils-Graphene Oxide Hybrid Organic Aerogels. ACS Appl. Mater. Interfaces 2013, 5, 5969-5975.

[93] Cheng, C.; Deng, J.; Lei, B.; He, A.; Zhang, X.; Ma, L.; Li, S.; Zhao, C. Toward 3D Graphene Oxide Gels Based Adsorbents for High-Efficient Water Treatment via the Promotion of Biopolymers. J. Hazard. Mater. 2013, 263, 467-478.

[94] Cheng, J.-S.; Du, J.; Zhu, W. Facile Synthesis of Three-Dimensional Chitosan–Graphene Mesostructures for Reactive Black 5 Removal. Carbohyd. Polym. 2012, 88, 61-67.

[95] Wang, J.; Zhao, G.; Jing, L.; Peng, X.; Li, Y. Facile Self-Assembly of Magnetite Nanoparticles on Three-Dimensional Graphene Oxide-Chitosan Composite for Lipase Immobilization. Biochem. Eng. J. 2015, 98, 75-83.

[96] Zhang, Y.; Liu, J.-W.; Chen, X.-W.; Wang, J.-H. A Three-Dimensional Amylopectin-Reduced Graphene Oxide Framework for Efficient Adsorption and Removal of Hemoglobin. J. Mater. Chem. B 2015, 3, 983-989.

[97] Liu, W.; Li, H.; Zeng, Q.; Duan, H.; Guo, Y.; Liu, X.; Sun, C.; Liu, H. Fabrication of Ultralight Three-Dimensional Graphene Networks with Strong Electromagnetic Wave Absorption Properties. J. Mater. Chem. A 2015, 3, 3739-3747.

[98] Wang, C.; Han, X.; Xu, P.; Zhang, X.; Du, Y.; Hu, S.; Wang, J.; Wang, X. The Electromagnetic Property of Chemically Reduced Graphene Oxide and Its Application As Microwave Absorping Material. Appl. Phys. Lett. 2011, 98, 072906.

[99] Ren, Y.; Zhu, C.; Qi, L.; Gao, H.; Chen, Y. Growth of ã-Fe2O3 Nanosheet Arrays on Graphene for Electromagnetic Absorption Applications. RSC Adv. 2014, 4, 21510-21516.

[100] Yu, H.; Wang, T.; Wen, B.; Lu, M.; Xu, Z.; Zhu, C.; Chen, Y.; Xue, X.; Sun, C.; Cao, M. Graphene/ Polyaniline Nanorod Arrays: Synthesis and Excellent Electromagnetic Absorption Properties. J. Mater. Chem. 2012, 22, 21679-21685.

[101] Wu, F.; Wang, Y.; Wang, M. Using Organic Solvent Absorption As a Self-Assembly Method to Synthesize Three-Dimensional (3D) Reduced Graphene Oxide (RGO)/Poly(3,4-ethylenedioxythiophene) (PEDOT) Architecture and Its Electromagnetic Absorption Properties. RSC Adv. 2014, 4, 49780-49782.

[102] Simon, P.; Gogotsi, Y. Materials for Electrochemical Capacitors. Nat. Mater. 2008, 7, 845-854.

[103] Mao, S.; Lu, G.; Chen, J. Three-Dimensional Graphene-Based Composites for Energy Applications. Nanoscale 2015, 7, 6924-6943.

[104] Zhai, T.; Lu, X.; Wang, H.; Wang, G.; Mathis, T.; Liu, T.; Li, C.; Tong, Y.; Li, Y. An Electrochemical Capacitor with Applicable Energy Density of 7.4 Wh/kg at Average Power Density of 3000 W/kg. Nano Lett. 2015, 15, 3189-3194.

[105] Ye, S.; Feng, J.; Wu, P. Deposition of Three-Dimensional Graphene Aerogel on Nickel Foam As a Binder-Free Supercapacitor Electrode. ACS Appl. Mater. Interfaces 2013, 5, 7122-7129.

[106] Song, Y.; Liu, T.-Y.; Xu, X.-X.; Feng, D.-Y.; Li, Y.; Liu, X.-X. Pushing the Cycling Stability Limit of Polypyrrole for Supercapacitors. Adv. Funct. Mater. 2015, 25, 4626-4632.

[107] Tai, Z.; Yan, X.; Xue, Q. Three-Dimensional Graphene/Polyaniline Composite Hydrogel As Supercapacitor Electrode. J. Electrochem. Soc. 2012, 159, A1702-A1709.

[108] Chen, C.; Fu, X.; Ma, T.; Fan, W.; Wang, Z.; Miao, S. Synthesis and Electrochemical Properties of Graphene Oxide/Nanosulfur/Polypyrrole Ternary Nanocomposite Hydrogel for Supercapacitors. J. Appl. Polym. Sci. 2014, 131, 9621-9625.

[109] Liu, H.; Wang, Y.; Gou, X.; Qi, T.; Yang, J.; Ding, Y. Three-Dimensional Graphene/Polyaniline Composite Material for High-Performance Supercapacitor Applications. Mater. Sci. Eng. B 2013, 178, 293-298.

[110] Wang, J.; Xian, H.; Peng, T.; Sun, H.; Zheng, F. Three-Dimensional Graphene-Wrapped PANI Nanofiber Composite As Electrode Material for Supercapacitors. RSC Adv. 2015, 5, 13607-13612.

[111] Bora, C.; Dolui, S. K. Fabrication of Polypyrrole/Graphene Oxide Nanocomposites by Liquid/Liquid Interfacial Polymerization and Evaluation of Their Optical, Electrical and Electrochemical Properties. Polymer 2012, 53, 923-932.

[112] Kulkarni, S. B.; Patil, U. M.; Shackery, I.; Sohn, J. S.; Lee, S.; Park, B.; Jun, S. High-Performance Supercapacitor Electrode Based on a Polyaniline Nanofibers/3D Graphene Framework As an Efficient Charge Transporter. J. Mater. Chem. A 2014, 2, 4989-4998.

[113] Lai, X.; Halpert, J. E.; Wang, D. Recent Advances in Micro-/Nano-Structured Hollow Spheres for Energy Applications: From Simple to Complex Systems. Energy Environ. Sci. 2012, 5, 5604-5618.

[114] Chen, H.; Zhou, S.; Chen, M.; Wu, L. Reduced Graphene Oxide–MnO2 Hollow Sphere Hybrid Nanostructures As High-Performance Electrochemical Capacitors. J. Mater. Chem. 2012, 22, 25207-25216.

[115] Dong, X.; Wang, J.; Wang, J.; Chan-Park, M. B.; Li, X.; Wang, L.; Huang, W.; Chen, P. Supercapacitor Electrode Based on Three-Dimensional Graphene-Polyaniline Hybrid. Mater. Chem. Phys. 2012, 134, 576-580.

[116] Zhang, J.; Wang, J.; Yang, J.; Wang, Y.; Chan-Park, M. B. Three-Dimensional Macroporous Graphene Foam Filled with Mesoporous Polyaniline Network for High Areal Capacitance. ACS Sustainable Chem. Eng. 2014, 2, 2291-2296.

[117] Pu, J.; Wang, X.; Zhang, T.; Li, S.; Liu, J.; Komvopoulos, K. High-Energy-Density, All-SolidState Microsupercapacitors with Three-Dimensional Interdigital Electrodes of Carbon/Polymer Electrolyte Composite. Nanotechnology, 2016, 27, 045701.

[118] Yu, P.; Zhao, X.; Huang, Z.; Li, Y.; Zhang, Q. Free-Standing Three-Dimensional Graphene and Polyaniline Nanowire Arrays Hybrid Foams for High-Performance Flexible and Lightweight Supercapacitors. J. Mater. Chem. A 2014, 2, 14413-14420.

[119] Chi, K.; Zhang, Z.; Xi, J.; Huang, Y.; Xiao, F.; Wang, S.; Liu, Y. Freestanding Graphene Paper Supported Three-Dimensional Porous Graphene–Polyaniline Nanocomposite Synthesized by Inkjet Printing and in Flexible All-Solid-State Supercapacitor. ACS Appl. Mater. Interfaces 2014, 6, 16312- 16319.

[120] Oren,Y. Capacitive Delonization (CDI) for Desalination and Water Treatment-Past, Present and Future (a Review). Desalination 2008, 228, 10-29.

[121] Yong, Y.-C.; Dong, X.-C.; Chan-Park, M. B.; Song, H.; Chen, P. Macroporous and Monolithic Anode Based on Polyaniline Hybridized Three-Dimensional Graphene for High-Performance Microbial Fuel Cells. ACS Nano 2012, 6, 2394-2400.

[122] Li, S.; Shu, K.; Zhao, C.; Wang, C.; Guo, Z.; Wallace, G.; Liu, H. K. One-Step Synthesis of Graphene/ Polypyrrole Nanofiber Composites As Cathode Material for a Biocompatible Zinc/Polymer Battery. ACS Appl. Mater. Interfaces 2014, 6, 16679-16686.

[123] Zhang, J.; Li, R.; Li, Z.; Liu, J.; Gu, Z.; Wang, G. Synthesis of Nitrogen-Doped Activated Graphene Aerogel/Gold Nanoparticles and Its Application for Electrochemical Detection of Hydroquinone and ODihydroxybenzene. Nanoscale 2014, 6, 5458-5466.

[124] Zhang, Z.; Fu, X.; Li, K.; Liu, R.; Peng, D.; He, L.; Wang, M.; Zhang, H.; Zhou, L. One-Step Fabrication of Electrochemical Biosensor Based on DNA-Modified Three-Dimensional ReducedGraphene Oxide and Chitosan Nanocomposite for Highly Sensitive Detection of Hg(II). Sensor. Actuat. B-Chem. 2016, 225, 453-462.

[125] Zhao, Z.-Q.; Chen, X.; Yang, Q.; Liu, J.-H.; Huang, X.-J. Selective Adsorption Toward Toxic Metal Ions Results in Selective Response: Electrochemical Studies on a Polypyrrole/Reduced Graphene Oxide Nanocomposite. Chem. Commun. 2012, 48, 2180-2182.

[126] Yang, Y.; Kang, M.; Fang, S.; Wang, M.; He, L.; Zhao, J.; Zhang, H.; Zhang, Z. Electrochemical Biosensor Based on Three-Dimensional Reduced Graphene Oxide and Polyaniline Nanocomposite for Selective Detection of Mercury Ions. Sensor. Actuat. B-Chem. 2015, 214, 63-69.

[127] Yang, T.; Guan, Q.; Li, Q.; Meng, L.; Wang, L.; Liu, C.; Jiao, K. Large-Area, Three-Dimensional Interconnected Graphene Oxide Intercalated with Self-Doped Polyaniline Nanofibers As a Free-Standing Electrocatalytic Platform for Adenine and Guanine. J. Mater. Chem. B 2013, 1, 2926-2933.

[128] Liu, J.; Wang, X.; Wang, T.; Li, D.; Xi, F.; Wang, J.; Wang, E. Functionalization of Monolithic and Porous Three-Dimensional Graphene by One-Step Chitosan Electrodeposition for Enzymatic Biosensor. ACS Appl. Mater. Interfaces 2014, 6, 19997-20002.

[129] Liu, J.; He, Z.; Xue, J.; Tan, T. T. Y. A Metal-Catalyst Free, Flexible and Free-Standing Chitosan/Vacuum-Stripped Graphene/Polypyrrole Three Dimensional Electrode Interface for High Performance Dopamine Sensing. J. Mater. Chem. B 2014, 2, 2478-2482.

[130] Yu, D.; Zeng, Y.; Qi, Y.; Zhou, T.; Shi, G. A Novel Electrochemical Sensor for Determination of Dopamine Based on AuNPs@SiO2 Core-Shell Imprinted Composite. Biosens. Bioelectron. 2012, 38, 270-277.

[131] Hu, H.; Zhao, Z.; Zhang, R.; Bin, Y.;Qiu, J. Polymer Casting of Ultralight Graphene Aerogels for The Production of Conductive Nanocomposites with Low Filling Content. J. Mater. Chem. A 2014, 2, 3756-3760.

[132] Zheng, Q.; Li, Z.; Yang, J.; Kim, J.-K. Graphene Oxide-Based Transparent Conductive Films. Prog. Mater. Sci. 2014, 64, 200-247.

[133] Fan, Z.; Gong, F.; Nguyen, S. T.; Duong, H. M. Advanced Multifunctional Graphene Aerogel-Poly (Methyl Methacrylate) Composites: Experiments and Modeling. Carbon 2015, 81, 396-404.

[134] Wang, Z.; Shen, X.; Garakani, M. A.; Lin, X.; Wu, Y.; Liu, X.; Sun, X.; Kim, J.-K. Graphene Aerogel/Epoxy Composites with Exceptional Anisotropic Structure and Properties. ACS Appl. Mater. Interfaces 2015, 7, 5538-5549.

[135] Chen, M.; Zhang, L.; Duan, S.; Jing, S.; Jiang, H.; Li, C. Highly Stretchable Conductors Integrated with a Conductive Carbon Nanotube/Graphene Network and 3D Porous Poly(dimethylsiloxane). Adv. Funct. Mater. 2014, 24, 7548-7556.

[136] Zhu, C.; Guo, S.; Fang, Y.; Dong, S. Reducing Sugar: New Functional Molecules for the Green Synthesis of Graphene Nanosheets. ACS Nano 2010, 4, 2429-2437.

[137] Chen, Z.; Ren, W.; Gao, L.; Liu, B.; Pei, S.; Cheng, H.-M. Three-Dimensional Flexible and Conductive Interconnected Graphene Networks Grown by Chemical Vapour Deposition. Nat. Mater. 2011, 10, 424-428.

[138] Chen, M.; Duan, S.; Zhang, L.; Wang, Z.; Li, C. Three-Dimensional Porous Stretchable and Conductive Polymer Composites Based on Graphene Networks Grown by Chemical Vapour Deposition and PEDOT:PSS Coating. Chem. Commun. 2015, 51, 3169-3172.

[139] Zhang, L.; Chen, G.; Hedhili, M. N.; Zhang, H.; Wang, P. Three-Dimensional Assemblies of Graphene Prepared by a Novel Chemical Reduction-Induced Self-Assembly Method. Nanoscale 2012, 4, 7038-7045.

[140] Xu, R.; Lu, Y.; Jiang, C.; Chen, J.; Mao, P.; Gao, G.; Zhang, L.; Wu, S. Facile Fabrication of Three-Dimensional Graphene Foam/Poly(dimethylsiloxane) Composites and Their Potential Application As Strain Sensor. ACS Appl. Mater. Interfaces 2014, 6, 13455-13460.

[141] Kashani, H.; Chen, L.; Ito, Y.; Han, J.; Hirata, A.; Chen, M. Bicontinuous Nanotubular GraphenePolypyrrole Hybrid for High Performance Flexible Supercapacitors. Nano Energy 2016, 19, 391-400.